Supporting Information

Triggered Drug Release from an Antibody Drug Conjugate using Fast "Click-to-Release" Chemistry in Mice

Raffaella Rossin,[†] Sander M.J. van Duijnhoven,[†] Wolter ten Hoeve,[‡] Henk M. Janssen,[§] Freek J.M. Hoeben,[§] Ron M. Versteegen,[§] Marc S. Robillard[†]*

[†] Tagworks Pharmaceuticals, High Tech Campus 11, 5656 AE Eindhoven, The Netherlands

[‡] Syncom, Kadijk 3, 9747 AT Groningen, The Netherlands

[§] SyMO-Chem, Het Kranenveld 14, 5612 AZ Eindhoven, The Netherlands

Table of Contents

Section S1: General procedures

Materials. All reagents, chemicals, materials and solvents were obtained from commercial sources, and were used as received: Biosolve, Merck and Cambridge Isotope Laboratories for (deuterated) solvents, and Aldrich, Acros, ABCR, Merck and Fluka for chemicals, materials and reagents. All solvents were of AR quality. Doxorubicin (Dox) and daunorubicin (Daun) hydrochloride were obtained from Avachem Scientific. Amine-functional dextran (MW=10 kDa) was obtained from Invitrogen. [^{177}Lu]Lutetium chloride and sodium [^{125}I]iodide solutions were purchased from Perkin Elmer. The Bolton-Hunter reagent (N-succinimidyl-3-[4-hydroxyphenyl]propionate), gelcode blue protein staining solutions and Zeba desalting spin columns (40 kDa MW cut-off, 0.5 mL) were purchased from Pierce Protein Research (Thermo Fisher Scientific). Amicon Ultra centrifugal filter units (30 and 50 MW cut-off) were purchased from Millipore. Tablets for the preparation of phosphate buffered saline solution (PBS) were purchased from Calbiochem. Mouse serum (MS) was purchased from Innovative Research. CC49 was produced from the ATCC hybridoma and purified as previously described.[1] Water was distilled and deionized (18 MΩcm) by means of a milli-Q water filtration system (Millipore).

Methods. ^{1}H NMR and ^{13}C NMR spectra were recorded on a Varian Mercury (300 and 400 MHz for ^{1}H NMR and 100 MHz for ^{13}C NMR) spectrometer or a Varian Unity Inova 500 MHz spectrometer (500 MHz for ^{1}H NMR). Chemical shifts are reported in ppm downfield from TMS at RT. Abbreviations used for splitting patterns are s=singlet, t=triplet, q=quartet, m=multiplet and br=broad. IR spectra were recorded on a Perkin Elmer 1600 FT-IR (UATR). Melting points were determined on a Büchi B-540 Melting Point apparatus. HPLC-MS/PDA was performed using a Shimadzu LC-10 AD VP series HPLC coupled to a diode array detector (Finnigan Surveyor PDA Plus detector, Thermo Electron Corporation) and an Ion-Trap (LCQ Fleet, Thermo Scientific). Analyses were performed using an Alltech Alltima HP C_{18} 3µ column using an injection volume of 1-4 µL, a flow rate of 0.2 mL/min and typically a gradient (5% to 100% in 10 min, held at 100% for 3 min) of MeCN in H_2O (both containing 0.1% formic acid) at 25 °C. Preparative RP-HPLC (MeCN / H_2O with 0.1% formic acid) was performed using a Shimadzu SCL-10A VP coupled to two Shimadzu LC-8A pumps and a Shimadzu SPD-10AV VP UV-vis detector on a Phenomenex Gemini 5µ C_{18} 110A column. HRMS was performed on either a Waters Acquity LC, that is equipped with a Sample Manager and Xevo G2 Qtof detector using Zspray lockspray ionisation, or a Bruker autoflex speed MALDI-TOF mass spectrometer (positive mode with DCTB as matrix). Mass deviations from the theoretical mass were typically between 0 and 2 ppm. RP-HPLC analysis of samples containing Dox/Daun was performed using an Agilent 1100 system equipped with an autosampler and a fluorescence detector. The samples were loaded on an Agilent Eclipse XDB-C_{18} column (4.6 × 150mm, 5µ), which was eluted at 1 mL/min with 30% MeCN in water containing 0.1% TFA. The drugs were detected at 590 nm with a fluorescent detector (upon excitation at 485 nm). Size exclusion (SEC)-HPLC was carried out on an Agilent 1200 system equipped with a Gabi radioactive detector. The samples were

loaded on a BioSep-S-3000 column (300×7.8 mm, 5 µ, Phenomenex) and eluted with 0.1 M phosphate buffer containing 0.15 M NaCl, pH 6.6, at 0.8-1 mL/min. The UV wavelength was preset at 260/280 nm or at 260/480 nm (Dox detection). SDS-PAGE was performed on a Phastgel system using 7.5% PAGE homogeneous and 4-15% PAGE gradient gels (GE Healthcare Life Sciences).

The drug-to-antibody ratio (DAR) for **12** was determined by UV-Vis measurements (Nanodrop) using 210000 M^{-1} cm^{-1} and 10400 M^{-1} cm^{-1} as extinction coefficients for CC49 (280 nm) and Dox (480 nm), respectively. The absorbance values were corrected for background and the A280 was further corrected for Dox contribution as follows

$$A_{280,corr} = A_{280} - 0.7324 \times A_{480}$$

where the correction factor was determined by measuring the absorbance of samples containing only free Dox.

Tetrazine titrations on CC49-TCO-Dox (**12**) solutions were performed by reacting the mAb (25 µg) with a known excess of carrier-added ^{177}Lu-**14** (20 min at 37 °C) in PBS (50 µL), followed by SDS-PAGE analysis and Phosphor Imager (Fuji FLA 7000). The amount of reacted tetrazine was quantified from the radioactivity % in the high MW portion of the gel and used to calculate the amount of available TCO in solution.

Section S2: Additional organic syntheses

3-(*tert*-butoxycarbonylaminomethyl)-6-methyl-1,2,4,5-tetrazine (24)

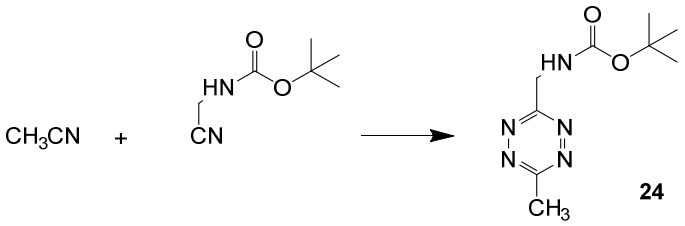

(*Tert*-butoxycarbonylamino)acetonitrile (620 mg; 3.97 mmol), nickel(II)triflate (680 mg; 1.90 mmol), MeCN (2.00 mL; 38.3 mmol), and hydrazine hydrate (9.2 mL; 190 mmol) were combined and stirred in an atmosphere of argon at 60 °C for 19 h. The mixture was cooled to RT, and all volatiles were removed in vacuo. The residue was suspended in THF (30 mL), acetic acid (70 mL) was added, and the mixture was cooled to 0 °C. Sodium nitrite (19.2 g; 278 mmol) was dissolved in water (50 mL), and added dropwise. After the addition, the mixture was stirred at 0 °C for 5 min, and then at 20 °C for an additional 15 min. Subsequently, all volatiles were remove in vacuo, and the residue was suspended in water (400 mL), and the product was extracted with chloroform (3×400 mL). The combined organic layers were dried with sodium sulfate, filtered over Celite, and concentrated. The crude product was purified by column chromatography on silica gel (20% EtOAc/chloroform) to give **24** as a pink solid (210 mg; 24%). ^{1}H-NMR (400 MHz, $CDCl_3$): δ=5.55 (br. s, 1H), 4.96 (d, *J*=6.0 Hz, 2H), 3.08 (s, 3H), 1.46 (s, 9H) ppm. LC-MS: *m/z* = +170.17 (calcd 170.07 for $C_5H_8N_5O_2^+$ [(*M*-tBu+H)$^+$]).

5-(((6-methyl-1,2,4,5-tetrazin-3-yl)methyl)amino)-5-oxopentanoic acid (26)

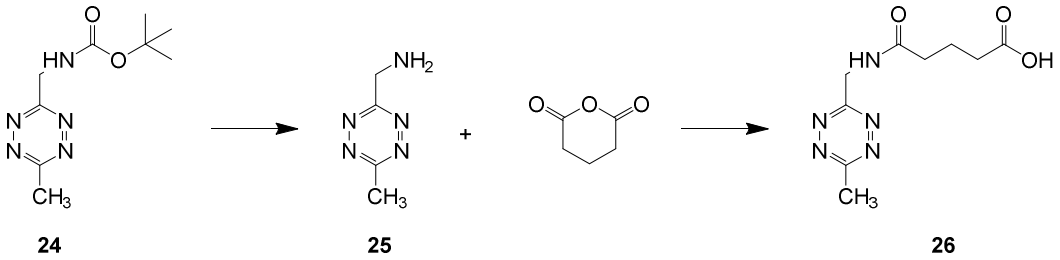

3-(*Tert*-butoxycarbonylaminomethyl)-6-methyl-1,2,4,5-tetrazine **24** (1.39 g; 6.17 mmol) was dissolved in methylene chloride (15 mL), and TFA (15 mL) was added. The mixture was stirred at RT under an atmosphere of argon for 1 h. Subsequently, the crude product **25** was dissolved in DMF (16 mL), and DIPEA (3.12 g; 24.2 mmol) and glutaric anhydride (780 mg; 6.84 mmol) were added. The mixture was stirred at RT under an atmosphere of argon for 1 h. All volatiles were removed in vacuo, and the crude product was redissolved in acetone, precipitated in diethyl ether (200 mL) at 0 °C, collected by

centrifugation, and thoroughly washed with diethyl ether. The residue was further purified by column chromatography on silica gel (4% MeOH/chloroform) to give **26** as a pink solid (1.28 g; 87%); mp 99 °C. ^{1}H-NMR (400 MHz, MeOD-d_4): δ=4.93 (s, 2H), 3.00 (s, 3H), 2.37 (td, *J* = 7.4, 3.9 Hz, 4H), 1.92 (t, *J* = 7.4 Hz, 2H) ppm. ^{13}C-NMR (100 MHz, MeOD-d_4): δ=175.2, 174.5, 168.0, 166.5, 41.8, 34.3, 32.4, 20.6, 19.6 ppm. HRMS (MALDI-TOF, *m/z*): Calcd for $C_9H_{14}N_5O_3^+$ ([*M*+H]$^+$): 240.1091, Found: 240.1084.

3,6-dimethyl-1,2,4,5-tetrazine functional dextran (5)

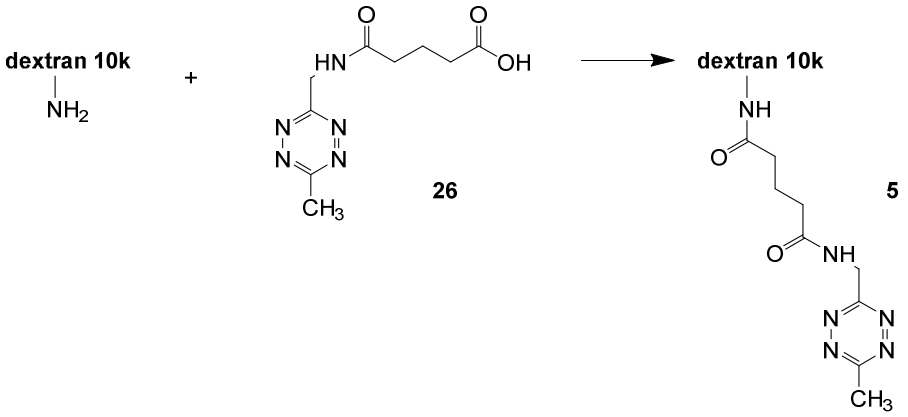

Amino-functional dextran (MW=10 kDa) (1.00 g; 0.25 mmol amine) was dissolved in DMSO (10 mL). DIPEA (161 mg; 1.25 mmol), 5-(((6-methyl-1,2,4,5-tetrazin-3-yl)methyl)amino)-5-oxopentanoic acid **26** (120 mg; 0.50 mmol), and PyBOP (325 mg; 6.25 mmol) were added, and the mixture was stirred for 90 min at 20 °C under an atmosphere of argon. The product was precipitated in ethanol (65 mL), collected by centrifugation, and thoroughly washed with ethanol. After removal of ethanol in vacuo, the precipitate was dissolved in water (25 mL), and the mixture was lyophilized to yield **5** as a pink solid (922 mg; 87%). By measuring the absorption at 520 nm and using a separately measured tetrazine extinction coefficient of 430 M^{-1} cm^{-1}, the average number of tetrazines was estimated to be 2.3 per dextran.

5-((6-cyanopyridin-3-yl)amino)-5-oxopentanoic acid (27)

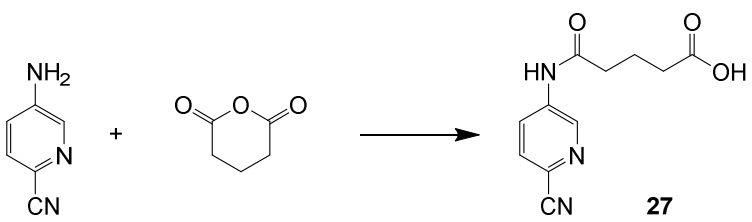

A solution of 5-amino-2-pyridine carbonitrile (1.00 g, 8.4 mmol) and glutaric anhydride (4.78 g, 41.9 mmol) in dry THF (ca. 20 mL) was stirred overnight under argon at 70 °C in a closed vessel. The suspension

was filtered to yield **27** as a solid (0.82 g; 42%); mp 234 °C. ^{1}H NMR (400 MHz, DMSO-d_6): δ=12.12 (s, 1H), 10.60 (s, 1H), 8.84 (d, *J*=2.4 Hz, 1H), 8.26 (dd, J_1=2.3 Hz, J_2=8.6 Hz, 1H), 7.97 (dd, *J*=8.5 Hz, 1H), 2.52-2.41 (m, 2H), 2.29 (t, *J*=7.3 Hz, 2H), 1.89-1.74 (m, 2H) ppm. ^{13}C NMR (100 MHz, DMSO-d_6): δ=174.1, 172.1, 141.7, 139.1, 129.6, 125.7, 125.6, 117.7, 35.4, 32.8, 20.0 ppm. HRMS (MALDI-TOF, *m/z*): Calcd for $C_{11}H_{12}N_3O_3^+$ ([*M*+H]$^+$): 234.0873, Found: 234.0880.

5-((6-(6-methyl-1,2,4,5-tetrazin-3-yl)pyridin-3-yl)amino)-5-oxopentanoic acid (28)

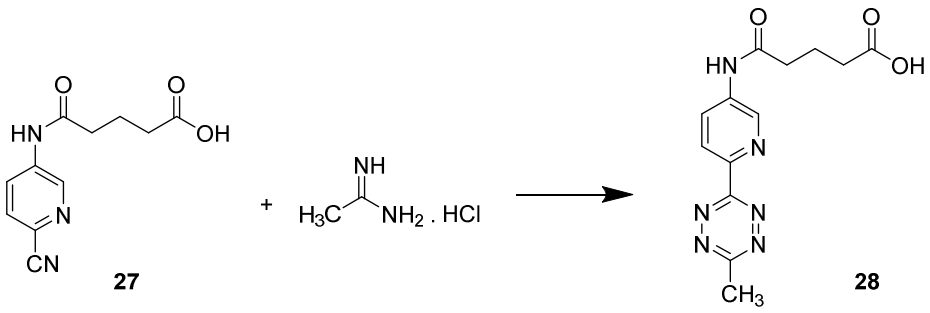

Hydrazine hydrate (1.09 mL, 22.2 mmol) was added to 5-((6-cyanopyridin-3-yl)amino)-5-oxopentanoic acid **27** (0.45 g, 1.93 mmol), acetamidine hydrochloride (0.80 g, 8.49 mmol) and sulfur (32 mg g, 0.97 mmol) in ethanol (5 mL) and the mixture was stirred overnight under argon at RT. The reaction mixture was concentrated and suspended in a mixture of THF (6 mL) and acetic acid (6 mL) over a cold-water bath. Sodium nitrite (1.2 g, 17.4 mmol in 5 mL water) was added dropwise and the mixture was stirred for another 5 min. Aqueous sodium hydrogen sulfate (50 mL 1M) and ethyl acetate (70 mL) were added and the layers were separated. The aqueous layer was extracted again with ethyl acetate (5×50 mL) and the combined organic fractions were washed with water (2×70 mL), dried with sodium sulfate, filtered, and concentrated. The crude material was recrystallized from chloroform/methanol to yield **28** as a pink solid (201 mg; 35%); mp 235 °C (dec). ^{1}H NMR (400 MHz, DMSO-d_6): δ=12.13 (s, 1H), 10.52 (s, 1H), 9.00 (d, *J*=2.4 Hz, 1H), 8.50 (d, *J*=8.6 Hz, 1H), 8.38 (dd, J_1=2.6 Hz, J_2=8.8 Hz, 1H), 3.01 (s, 3H), 2.51-2.45 (m, 2H), 2.33-2.30 (m, 2H), 1.89-1.82 (m, 2H) ppm. ^{13}C NMR (100 MHz, DMSO-d_6): δ=174.10, 171.87, 167.07, 162.69, 144.04, 141.06, 138.18, 126.16, 124.17, 35.36, 32.92, 20.85, 20.16 ppm. HRMS (MALDI-TOF, *m/z*): Calcd for $C_{13}H_{15}N_6O_3^+$ ([*M*+H]$^+$): 303.1200, Found: 303.1201.

3-(pyridin-2-yl)-6-methyl-1,2,4,5-tetrazine functional dextran (6)

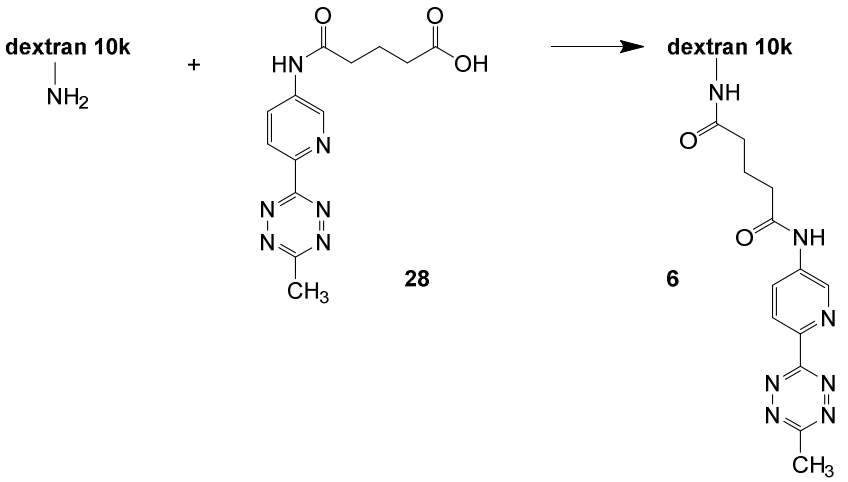

Amino-functional dextran (MW=10 kDa) (1.00 g; 0.25 mmol amine) was dissolved in DMSO (10 mL). 4-Methylmorpholine (253 mg; 2.50 mmol), 5-((6-(6-methyl-1,2,4,5-tetrazin-3-yl)pyridin-3-yl)amino)-5-oxopentanoic acid **28** (151 mg; 0.50 mmol), and PyBOP (325 mg; 6.25 mmol) were added, and the mixture was stirred for 1 h at 20 °C under an atmosphere of argon. The product was precipitated in ethanol (60 mL), collected by centrifugation, and thoroughly washed with ethanol. After removal of ethanol in vacuo, the precipitate was dissolved in water (15 mL), and the mixture was lyophilized to yield **6** as a pink solid (898 mg; 83%). By measuring the absorption at 520 nm and using a separately measured tetrazine extinction coefficient of 430 M^{-1} cm^{-1}, the average number of tetrazines was estimated to be 2.3 per dextran.

Section S3: Antibody conjugation and in vitro release studies

CC49-TCO-Dox (12) preparation

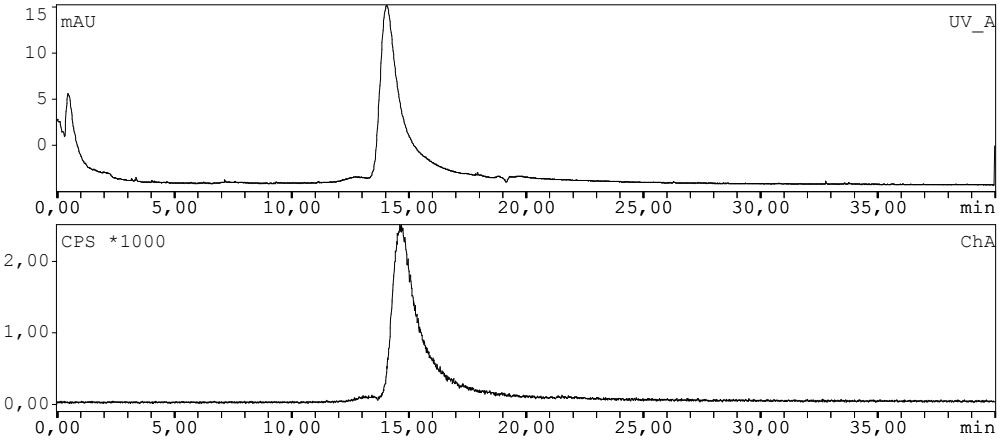

Figure S1: SEC-HPLC analysis of ^{125}I-CC49-TCO-Dox (top: UV profile at 260 nm; bottom: radioactivity profile).

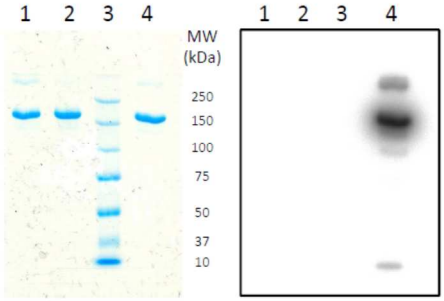

Figure S2: SDS-PAGE analysis (full-length gel, protein stain and radiogram) of (1) CC49, (2) CC49-TCO-Dox, (4) ^{125}I-CC49-TCO-Dox (Lane 3: protein MW standards).

Release of Doxorubicin from NHS-TCO-Doxorubicin (axial isomer 23a)

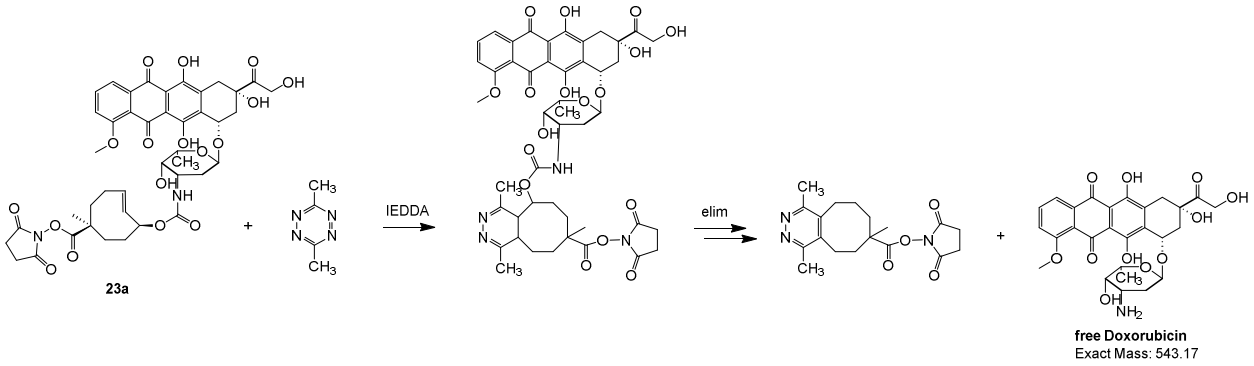

Figure S3: Dox release scheme

A solution of NHS-TCO-Dox (axial isomer **23a**) in DMSO (10 µL 2.5 mM; 2.5×10^{-8} mol) was diluted with 0.25 mL MeCN and 0.75 mL PBS buffer. A solution of 3,6-dimethyl tetrazine (**3**) in MeCN (10 µL 25 mM; 2.5×10^{-7} mol) was added, and the mixture was homogenized and kept at 37 °C for 60 min. HPLC-MS/PDA analysis of the mixture revealed the formation of free Dox, of which the retention time, MS-spectrum and UV-spectrum matched exactly with a control sample of Dox (see Section S7).

Doxorubicin release from CC49-TCO-Dox in vitro

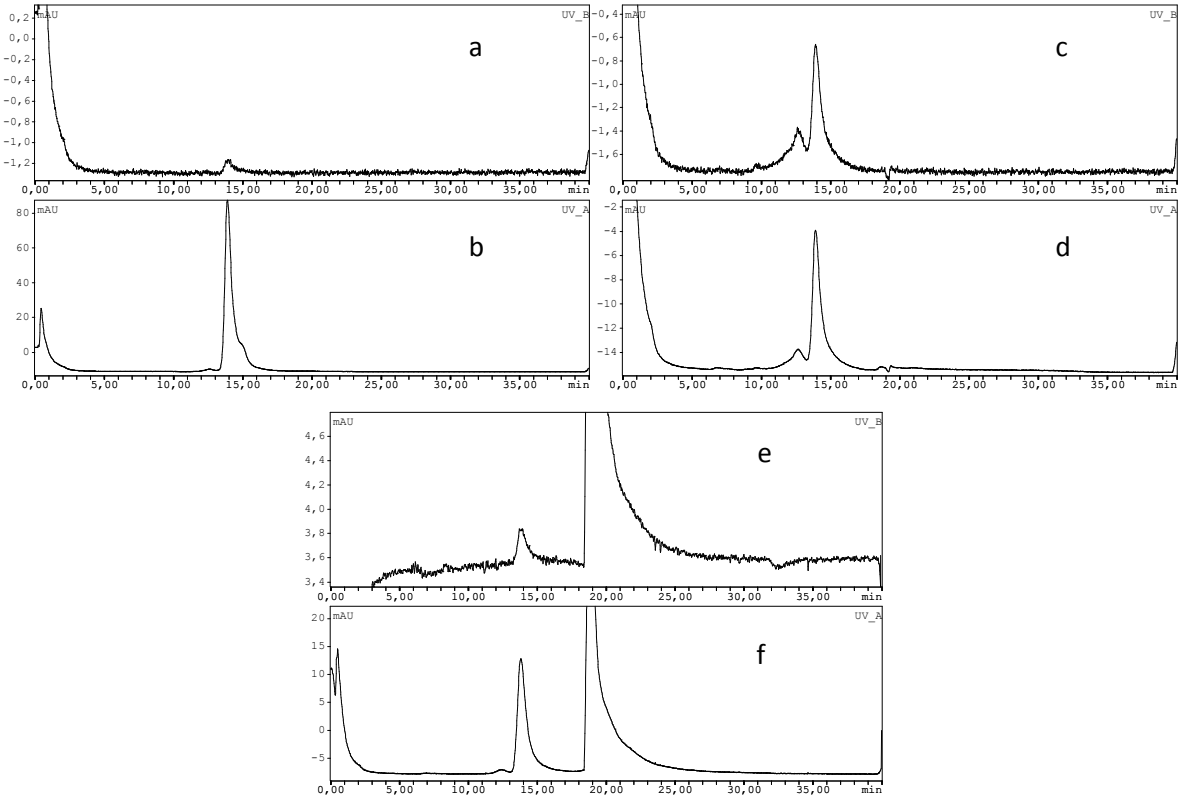

Figure S4: SEC-HPLC analysis: UV profiles of CC49 at (a) 480 nm and (b) 260 nm, CC49-TCO-Dox at (c) 480 nm and (d) 260 nm, and CC49-TCO-Dox/**3** mixure (24 h incubation in PBS at 37 °C) at (e) 480 nm and (f) 260 nm.

The absolute Dox release from **12** upon addition activator **3** was measured by SEC-HPLC in triplicate. At 1, 3 and 24 h an aliquot of the reaction mixture was analyzed by SEC with UV detection at 260 nm (protein) and 480 nm (Dox). The % release Dox was determined from the area ratio at 480 and 260 nm (A_{480}/A_{260}) for the mAb peak (R_t=13-15 min). Figure S4 shows examples of chromatograms for native CC49 (panels a,b; A_{480}/A_{260} = 0.0020±0.0002, corresponding to 100% release), unreacted **12** (panels c,d; A_{480}/A_{260} = 0.1502±0.0034, corresponding to 0% release) and a mixture of **12** and **3** after 24 h incubation in PBS (panels e,f; A_{480}/A_{260} = 0.0379±0.0003, corresponding to 76.1±0.2% release). The broad peak with R_t=19-25 min (panels e,f) is due to free Dox and activator **3**.

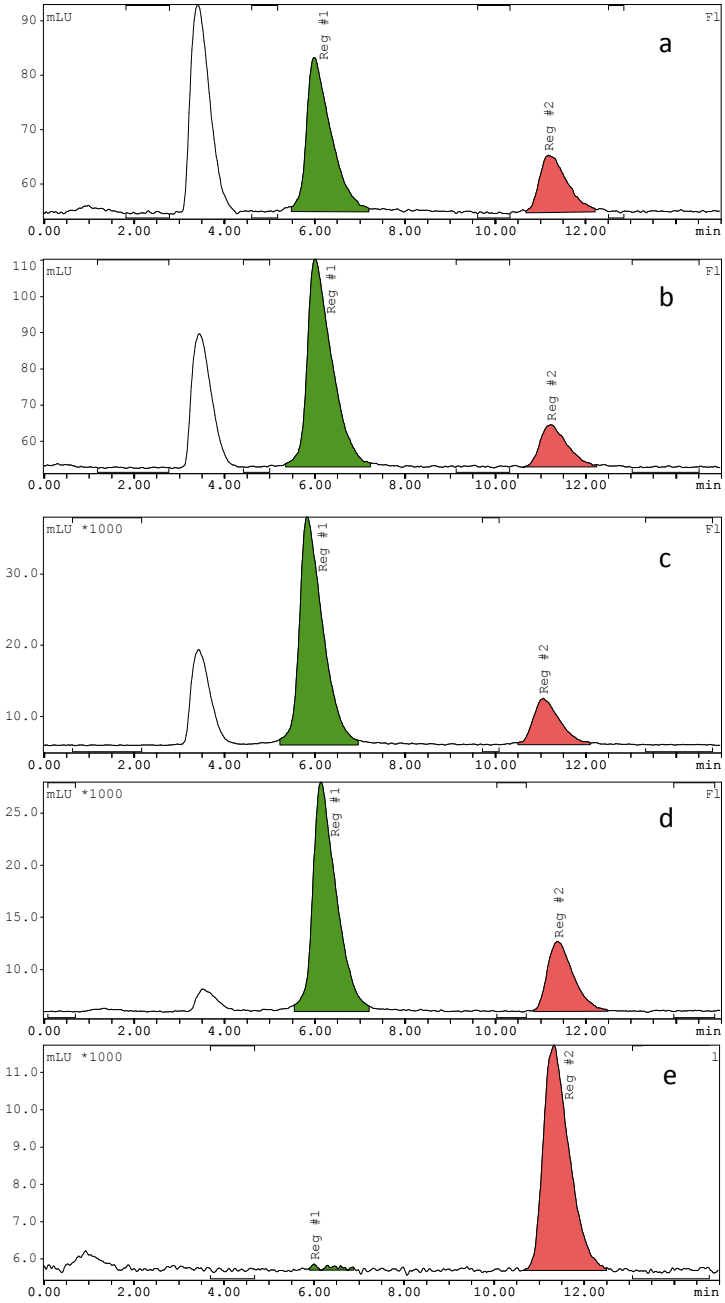

Figure S5: Examples of fluorescence RP-HPLC chromatograms of supernatants obtained from reaction mixtures incubated in PBS at 37 °C: (a, b, c) CC49-TCO-Dox/**3**/Daun at 1, 2 and 60 min; (d) CC49-TCO-Dox/**4**/Daun at 60 min; (e) CC49-TCO-Dox/Daun at 24 h (**3-4**: R_t = 3.5 min; Dox: R_t = 5.8 min; Daun: R_t = 11.0 min).

In 50% MS substantial Dox and Daun degradation was observed during incubation at 37 °C (Figure S6, peaks at R_t=3.0 and 9.3 min) therefore in this medium the experiments were carried out only up to 3 h incubation. Dox and Daun degradation is the likely cause for the apparent lower Dox release observed by RP-HPLC vs SEC-HPLC (apparent ca. 5% lower release) and in MS vs PBS (apparent ca. 10% lower Dox release) as shown in Figures 3a and Table S1.

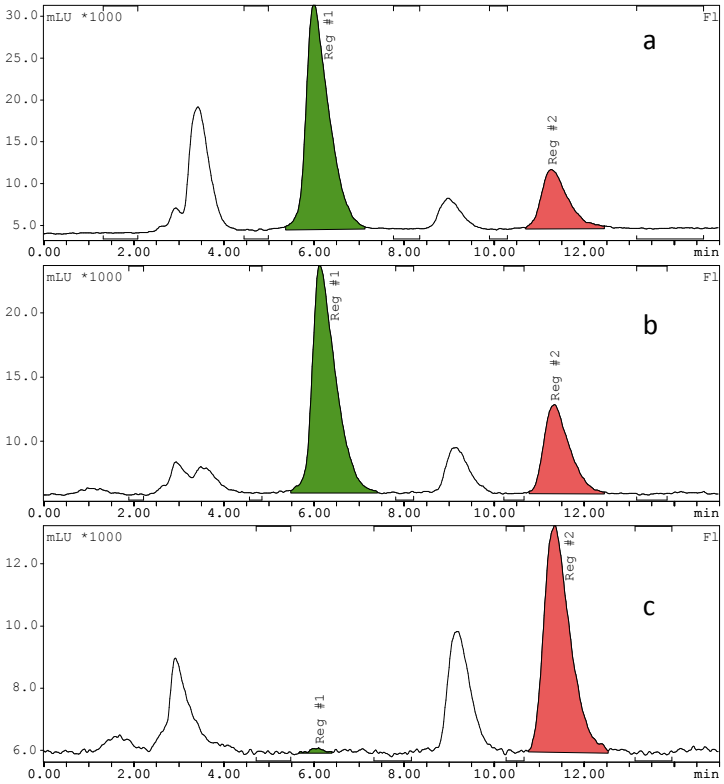

Figure S6: Examples of fluorescence RP-HPLC chromatograms of supernatants obtained from (a) CC49-TCO-Dox/**3**/Daun, (b) CC49-TCO-Dox/**4**/Daun and (c) CC49-TCO-Dox/Daun mixtures in 50% mouse serum after 1 h (a, b) and 3 h (c) incubation at 37 °C (**3-4**: R_t = 3.5 min; Dox: R_t = 5.8 min; Daun: R_t = 11.0 min; Dox/Daun degradation products: R_t=3.0 and 9.3 min).

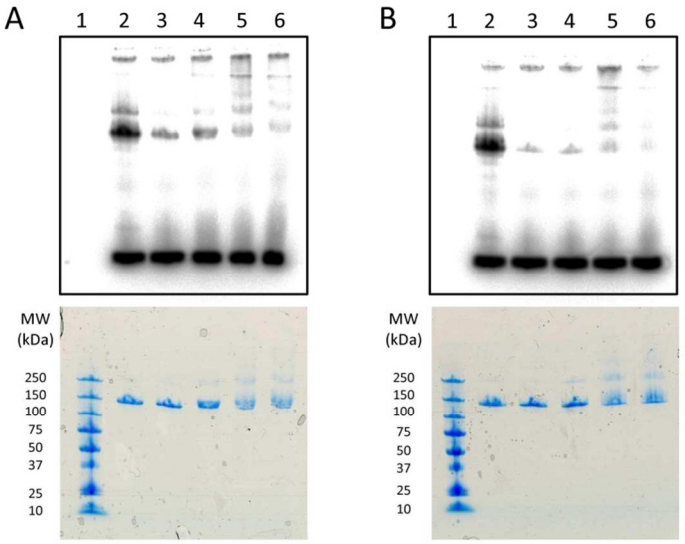

Figure S7: SDS-PAGE analysis (full length gels, radiogram and protein stain) of CC49-TCO-Dox/activator mixtures incubated for (A) 1 h and (B) 3 h at 37 °C in PBS followed by reaction with ^{177}Lu-DOTA-tetrazine (lane 1: protein MW standards; lane 2: CC49-TCO-Dox; lane 3: CC49-TCO-Dox + **3**; lane 4: CC49-TCO-Dox + **4**; lane 5: CC49-TCO-Dox + **5**; lane 6: CC49-TCO-Dox + **6**).

Table S1: Comparative time dependent Dox release from CC49-TCO-Dox (1 µM) upon reaction with activators **3-6** in PBS (extract of Figure 3a) and 50% MS as determined by RP-HPLC; amount of residual free TCO after 1 and 3 h incubation of CC49-TCO-Dox with activators **3-6** in PBS as determined by a titration with ^{177}Lu-DOTA-tetrazine (n=3).

activator	% Dox release in PBS				% Dox release in 50% MS			% free TCO in PBS	
	1 h	2 h	3 h	24 h	1 h	2 h	3 h	1 h	3 h
3	66.8±1.5	69.8±0.9	68.9±1.1	69.6±1.1	58.9±0.8	59.2±0.2	56.5±0.2	2.4±0.2	1.7±0.3
4	45.8±0.5	47.5±0.7	48.8±2.2	48.6±1.1	48.1±1.7	47.6±1.8	46.4±2.0	1.5±0.0	0.9±0.6
5	35.6±2.7	42.9±3.9	44.7±3.2	51.3±4.2	28.3±1.2	33.9±1.5	35.4±1.2	17.7±1.9	10.1±1.8
6	35.0±0.9	36.3±0.4	37.6±0.4	34.0±0.6	30.4±0.1	30.3±0.2	28.8±0.4	1.9±0.4	0.8±0.0

Section S4: Immunoreactivity

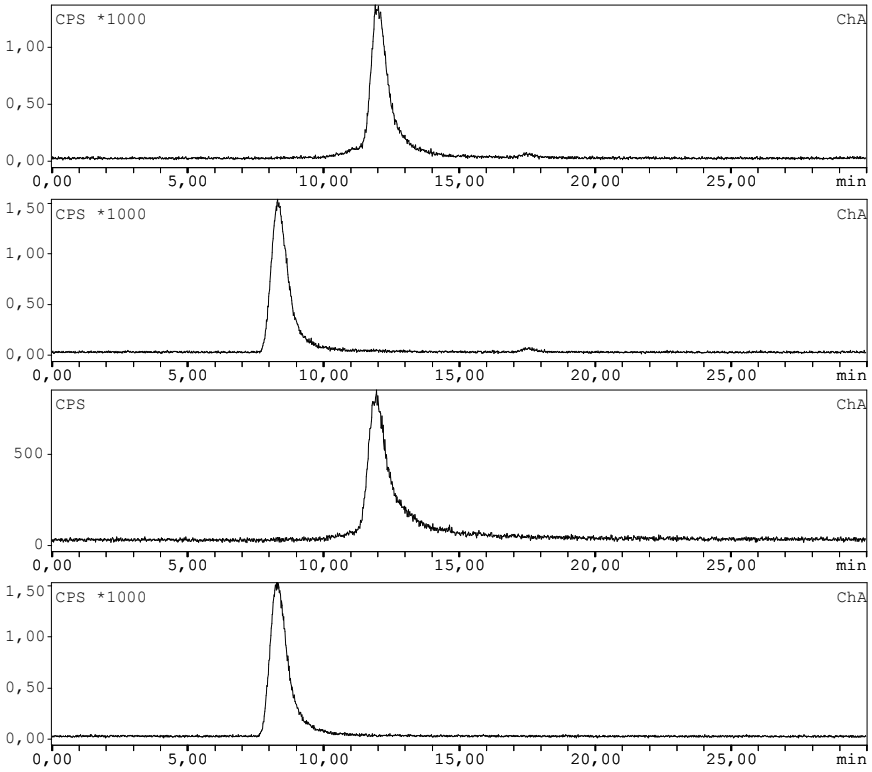

Figure S8: Immunoreactivity measurements: (from top to bottom) ^{125}I-CC49-TCO-Dox incubated in 1% bovine serum albumin (BSA) in PBS; ^{125}I-CC49-TCO-Dox incubated with 20 eq TAG72 positive bovine submaxillary mucin (BSM) in 1% BSA in PBS; ^{177}Lu-CC49-TCO-Dox incubated in 1% BSA in PBS; ^{177}Lu-CC49-TCO-Dox incubated with 20 eq BSM in 1% BSA in PBS.

Section S5: Animal experiments

Biodistribution in tumor-free mice

Table S2: Comparative biodistribution of ^{125}I-CC49-TCO-Dox (**12**) and ^{125}I-CC49 (from Rossin et al.[1]) in tumor free mice 4 days post-mAb injection. Data are presented as the mean ± SD (n=3).

	^{125}I-CC49-TCO-Dox	**^{125}I-CC49**
	%ID/g	
Blood	12.09 ± 0.30	12.33 ± 1.26
Heart	2.78 ± 0.33	3.92 ± 0.29
Lung	4.91 ± 0.82	5.13 ± 1.36
Liver	3.32 ± 0.17	3.17 ± 1.09
Spleen	2.54 ± 0.30	2.18 ± 0.92
Kidney (L)	3.44 ± 0.31	3.26 ± 0.86
Muscle	1.21 ± 0.22	1.24 ± 0.20
Bone	1.44 ± 0.07	1.15 ± 0.29
Brain	0.32 ± 0.09	0.46 ± 0.06
	%ID/organ	
Stomach	0.29 ± 0.01	0.26 ± 0.05
Intestine	2.14 ± 0.29	2.30 ± 0.34
Thyroid	0.66 ± 0.25	0.71 ± 0.07

Table S3: Pharmacokinetic parameters for ^{125}I-CC49-TCO-Dox (**12**) and ^{125}I-CC49 in tumor free mice

	$t_{1/2,\alpha}$ (h)	$\%_\alpha$	$t_{1/2,\beta}$ (h)	$t_{1/2}$ (h) [a]	C_{max} (µg/mL)
CC49	2.6	55	64.4	26.3	43.9
CC49-TCO-Dox	3.5	58	159.2	26.9	48.8

[a] $t_{1/2} = \ln 2 \times AUC/C_{max}$

Biodistribution in tumor bearing mice

Similar ^{125}I-**12** uptake in tumors was found in all animal groups (Table S4) signifying that the differences ^{177}Lu-**14** uptakes in these tumors (Figure 4 and Table S5) were caused by different reaction yields between TCO and activators **3-6**. Beside tumor, ^{125}I-**12** was diffusely distributed in all organs and tissues. The relatively high levels of ^{125}I-radioactivity in blood are likely due to the presence of non-TCO functionalized CC49 in the mAb preparation which did not react with the clearing agent. In fact, beside tumor and kidney (renal excretion), in the "no activator" group very low ^{177}Lu-**14** uptake was observed in

blood and non-target organs, signifying that the clearing agent successfully removed all CC49-TCO-Dox from the circulation, as previously observed for other TCO-functionalized mAb constructs.[1-2]

Table S4: ^{125}I-CC49-TCO-Dox (**12**) and ^{125}I-CC49 ("no ADC" group) biodistribution data from dual-isotope experiments. Data represent the mean ± SD.

	no activator	**3**	**3**	**3**	**4**	**4**	**4**	**5**	**5**	**6**	**no ADC**
organ		1x dose iv	10x dose iv	10x dose ip	1x dose iv	10x dose iv	10x dose ip	1x dose iv	10x dose iv	1x dose iv	
	n=6	n=4	n=4	n=4	n=4	n=4	n=4	n=3	n=3	n=4	n=4
						%ID/g					
blood	7.41±0.20	7.69±0.39	8.84±0.58	5.70±1.69	5.73±1.15	9.21±0.92	8.54±1.12	6.94±0.64	5.54±2.65	6.72±0.95	11.67±0.39
tumor	32.43±5.45	29.55±1.05	32.49±3.87	28.84±10.91	34.75±9.30	33.88±5.29	33.30±6.88	33.77±5.70	29.88±6.99	36.96±8.70	34.81±9.91
heart	2.19±0.75	2.25±0.35	2.21±0.14	1.62±0.44	1.65±0.29	2.19±0.36	2.53±0.91	1.97±0.09	1.60±0.74	1.74±0.18	2.61±0.35
lung	3.40±0.39	3.38±0.05	4.04±0.33	2.54±0.74	2.76±0.52	3.90±0.18	4.17±0.51	3.22±0.06	2.57±1.00	2.70±0.49	5.20±0.65
liver	5.36±0.45	5.13±1.00	5.51±0.88	3.70±0.43	4.20±0.75	4.98±1.22	6.08±0.60	4.92±0.73	6.83±2.84	6.27±0.80	5.19±0.82
spleen	2.43±0.73	2.16±0.45	2.41±1.16	1.70±0.35	1.27±0.18	2.17±0.94	2.44±0.44	2.21±0.87	1.96±0.77	2.04±0.89	2.61±0.43
kidney (R)	2.43±0.42	2.64±0.23	2.99±0.20	1.68±0.34	1.95±0.39	2.47±0.33	2.61±0.26	2.25±0.03	1.79±0.91	1.60±0.46	3.44±0.15
muscle	0.62±0.22	0.54±0.07	0.50±0.11	0.51±0.15	0.41±0.15	0.71±0.22	0.71±0.05	0.54±0.07	0.72±0.25	0.80±0.14	0.72±0.22
bone	1.13±0.22	1.03±0.10	1.06±0.13	0.68±0.20	0.84±0.32	0.92±0.18	0.97±0.12	0.96±0.20	0.80±0.27	0.85±0.39	1.29±0.14
						%ID/organ					
stomach	0.55±0.27	0.55±0.35	0.49±0.17	0.59±0.20	0.79±0.16	0.30±0.04	0.35±0.03	0.47±0.29	0.29±0.06	0.37±0.03	0.66±0.62
intestine	3.19±0.47	3.18±0.30	2.88±0.30	2.56±0.51	2.69±0.58	3.39±0.68	3.51±0.31	2.95±0.37	2.39±0.37	2.60±0.48	3.00±0.11
thyroid	0.79±0.55	0.82±0.17	0.81±0.25	1.08±0.52	1.61±0.59	1.06±0.22	0.38±0.06	0.76±0.08	0.44±0.04	0.52±0.20	0.80±0.29

Table S5: ^{177}Lu-DOTA-tetrazine (**14**) biodistribution data in mice pretreated with ^{125}I-CC49-TCO-Dox (**12**) and activators **3-6**, ^{125}I-CC49-TCO and no activator or^{125}I-CC49 ("no ADC" group), from dual-isotope experiments. Data represent the mean ± SD.

	no activator	**3**	**3**	**3**	**4**	**4**	**4**	**5**	**5**	**6**	**no ADC**
organ		1x dose iv	10x dose iv	10x dose ip	1x dose iv	10x dose iv	10x dose ip	1x dose iv	10x dose iv	1x dose iv	
	n=6	n=4	n=4	n=4	n=4	n=4	n=4	n=3	n=3	n=4	n=4
						%ID/g					
blood	0.08±0.02	0.07±0.01	0.03±0.00	0.03±0.00	0.01±0.00	0.01±0.01	0.02±0.00	0.05±0.01	0.05±0.01	0.03±0.00	0.03±0.01
tumor	1.23±0.34	1.13±0.28	0.87±0.51	0.61±0.43	0.38±0.08	0.42±0.13	0.43±0.13	0.50±0.04	0.18±0.03	0.11±0.05	0.08±0.02
heart	0.05±0.01	0.04±0.00	0.03±0.01	0.03±0.00	0.01±0.00	0.02±0.00	0.04±0.03	0.06±0.05	0.04±0.00	0.03±0.01	0.03±0.01
lung	0.19±0.05	0.15±0.02	0.11±0.00	0.10±0.04	0.05±0.00	0.04±0.01	0.05±0.01	0.23±0.05	0.26±0.03	0.14±0.06	0.14±0.02
liver	0.19±0.04	0.16±0.01	0.16±0.02	0.14±0.02	0.12±0.02	0.11±0.01	0.11±0.01	0.13±0.00	0.16±0.01	0.14±0.02	0.18±0.02
spleen	0.08±0.02	0.08±0.02	0.08±0.02	0.07±0.01	0.05±0.02	0.04±0.01	0.04±0.01	0.07±0.01	0.14±0.12	0.08±0.03	0.08±0.02
kidney (R)	1.55±0.39	1.46±0.05	1.42±0.13	1.31±0.34	1.07±0.21	0.92±0.12	0.87±0.13	1.22±0.17	1.48±0.01	1.30±0.19	1.47±0.35
muscle	0.02±0.010	0.01±0.00	0.01±0.00	0.02±0.00	0.01±0.00	0.01±0.00	0.01±0.00	0.02±0.01	0.03±0.02	0.05±0.06	0.01±0.01
bone	0.12±0.09	0.26±0.31	0.07±0.01	0.08±0.06	0.04±0.02	0.02±0.00	0.03±0.01	0.03±0.02	0.19±0.21	0.10±0.06	0.07±0.04
						%ID/organ					
stomach	0.02±0.01	0.03±0.01	0.03±0.04	0.09±0.14	0.04±0.02	0.01±0.01	0.01±0.01	0.03±0.02	0.02±0.00	0.01±0.00	0.04±0.05
intestine	0.31±0.14	0.38±0.14	0.40±0.17	0.56±0.16	0.63±0.41	0.34±0.17	0.73±0.59	0.28±0.10	0.24±0.05	0.34±0.20	0.64±0.29

Dox extraction from tissue samples

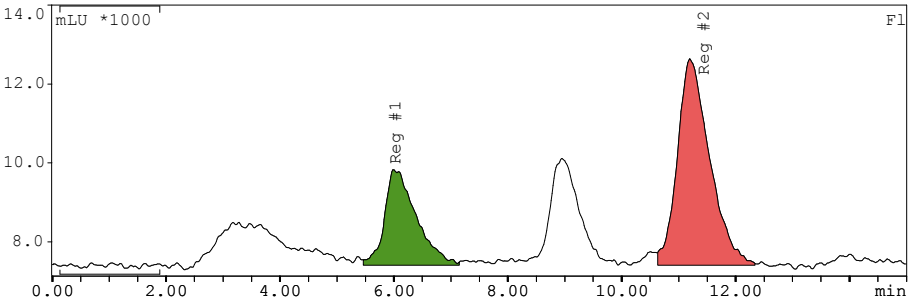

Figure S9: Example of fluorescence RP-HPLC chromatogram of the tumor extract obtained from a mouse belonging to the "**6**, 1x dose iv" group (Dox: R_t = 6.0 min; Daun: R_t = 11.2 min; Dox/Daun degradation products: R_t=3.2 and 9.0 min).

RP-HPLC analysis showed the presence of 71±30 and 50±6 pmol Dox/g at time of euthanasia (4 h post activator adiministration) in the tumors of the mice treated with **5** and **6**, respectively. These values correspond to 44±11% and 37±5% of the drug that was actually released from tumor-bound CC49-TCO-Dox based on ^{125}I-**12** uptake in tumor and in vitro tetrazine-induced release profiles in PBS. Considering the pronounced Dox degradation observed in vitro and in vivo and the fact that we only quantified the peak corresponding to intact Dox the actual amounts of released Dox in tumor are probably significantly higher. On the contrary, only 0.7±0.2% Dox (based on ^{125}I-**12** tumor uptake) was found in tumors that were not treated with tetrazine activators. These findings confirm tetrazine-triggered release of a TCO-bound drug in vivo and prove that a significant amount of the drug can be retained in the tumor in spite of the extracellular release mechanism. These results are on par with the levels of maytansine derivatives found in the tumors of mice treated with conventional ADCs, which rely on internalization and intracellular degradation for drug release. In those tumors, free drug / ADC ratios of up to 48% were reached 1-2 days after ADC administration.[3]

Section S6: References

(1) Rossin, R.; van Duijnhoven, S. M. J.; Läppchen, T.; van den Bosch, S. M. and Robillard, M. S. (2014) Trans-Cyclooctene Tag with Improved Properties for Tumor Pretargeting with the Diels–Alder Reaction. *Mol. Pharm. 11*, 3090-3096.

(2) Rossin, R.; Läppchen, T.; van den Bosch, S. M.; Laforest, R. and Robillard, M. S. (2013) Diels-Alder Reaction for Tumor Pretargeting: In Vivo Chemistry Can Boost Tumor Radiation Dose Compared with Directly Labeled Antibody. *J. Nucl. Med. 54*, 1989-1995.

(3) Erickson, H. K.; Lewis Phillips, G. D.; Leipold, D. D.; Provenzano, C. A.; Mai, E.; Johnson, H. A.; Gunter, B.; Audette, C. A.; Gupta, M.; Pinkas, J. et al. (2012) The Effect of Different Linkers on Target Cell Catabolism and Pharmacokinetics/Pharmacodynamics of Trastuzumab Maytansinoid Conjugates. *Mol. Cancer Ther. 11*, 1133-1142.

Section S7: Spectra

^{1}H-NMR spectrum of methyl *rel*-(1*S*,6*S*,4*E*,*pS*)-6-hydroxy-1-methylcyclooct-4-ene-1-carboxylate (equatorial isomer 20b) (500 MHz, $CDCl_3$)

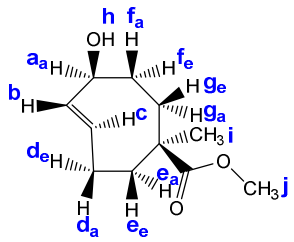

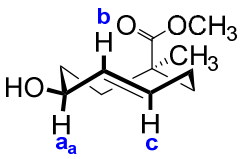

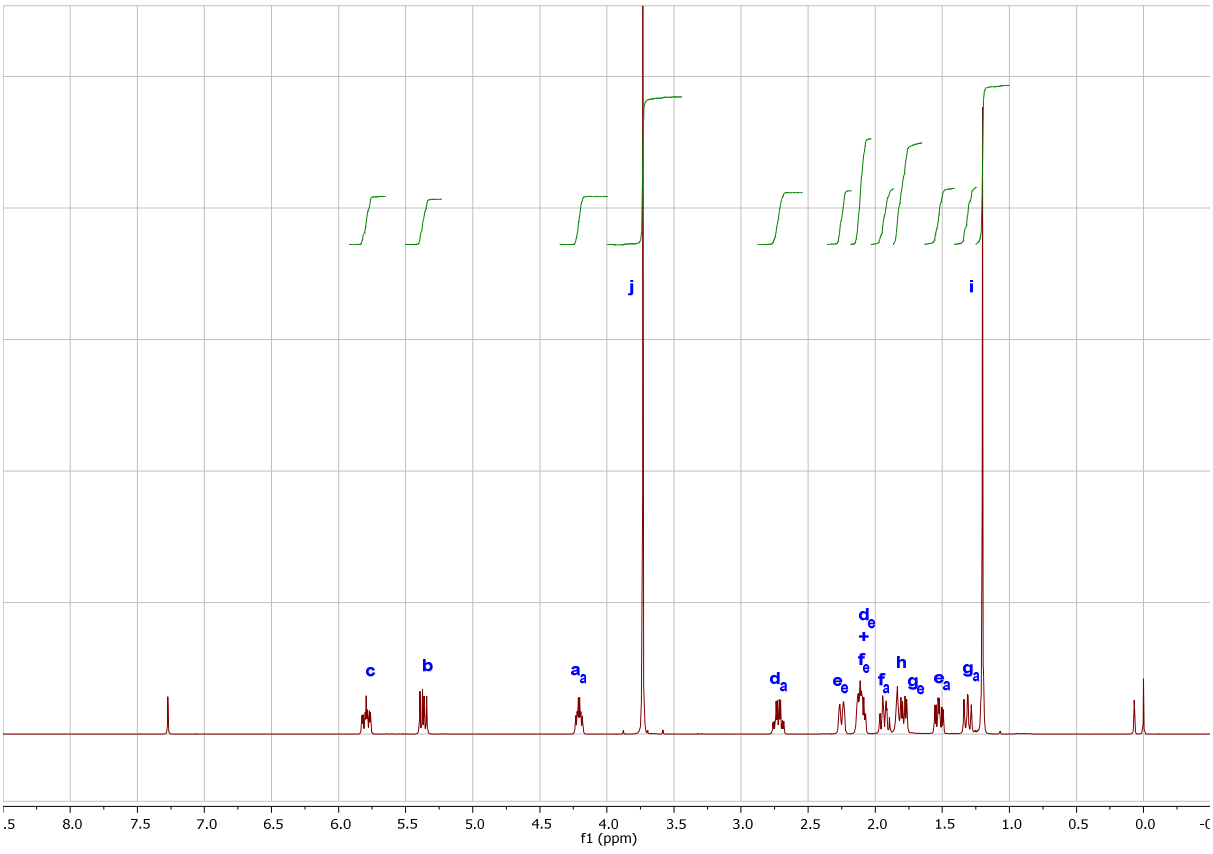

^{13}C-NMR spectrum of methyl *rel*-(1*S*,6*S*,4*E*,*pS*)-6-hydroxy-1-methylcyclooct-4-ene-1-carboxylate (equatorial isomer 20b) (125 MHz, $CDCl_3$)

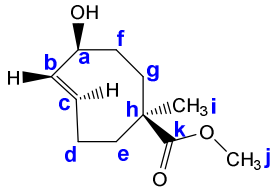

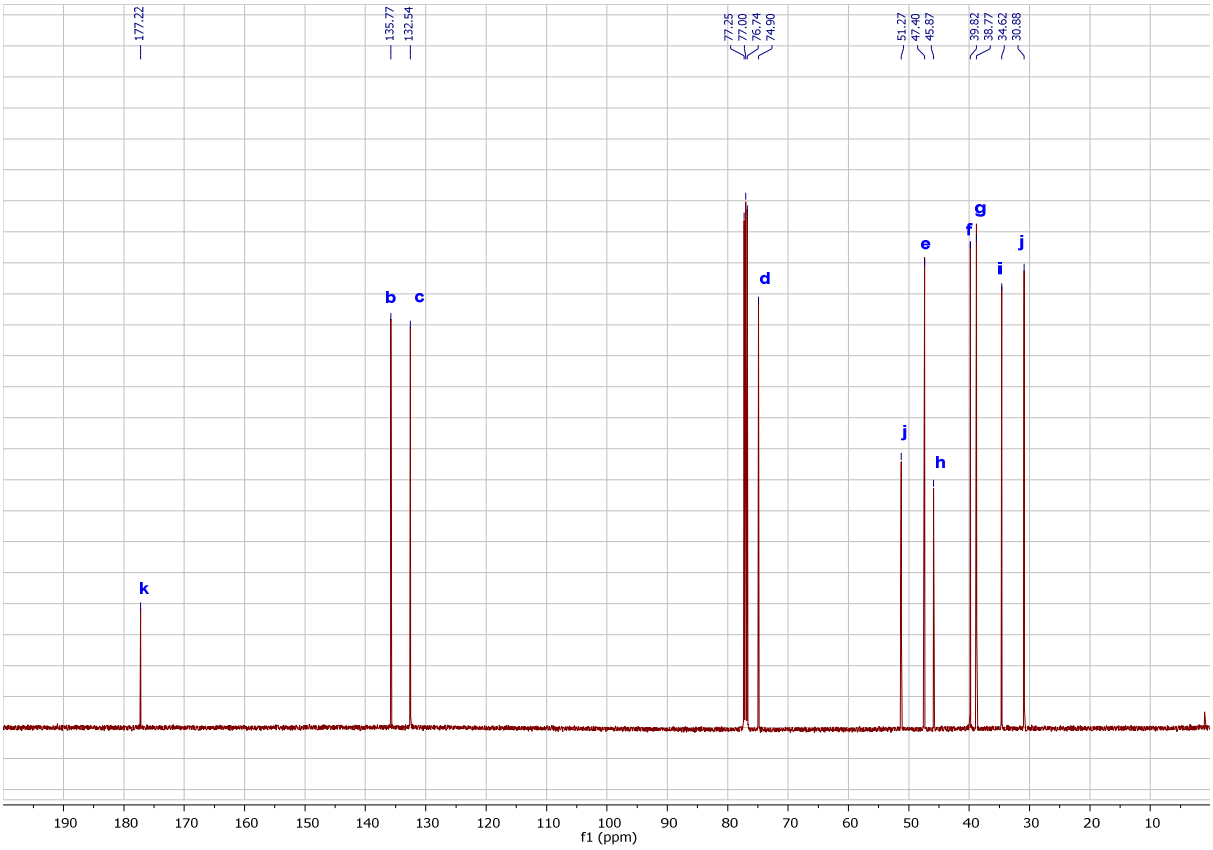

COSY spectrum of methyl *rel*-(1*S*,6*S*,4*E*,*pS*)-6-hydroxy-1-methylcyclooct-4-ene-1-carboxylate (equatorial isomer 20b) (500 MHz, $CDCl_3$)

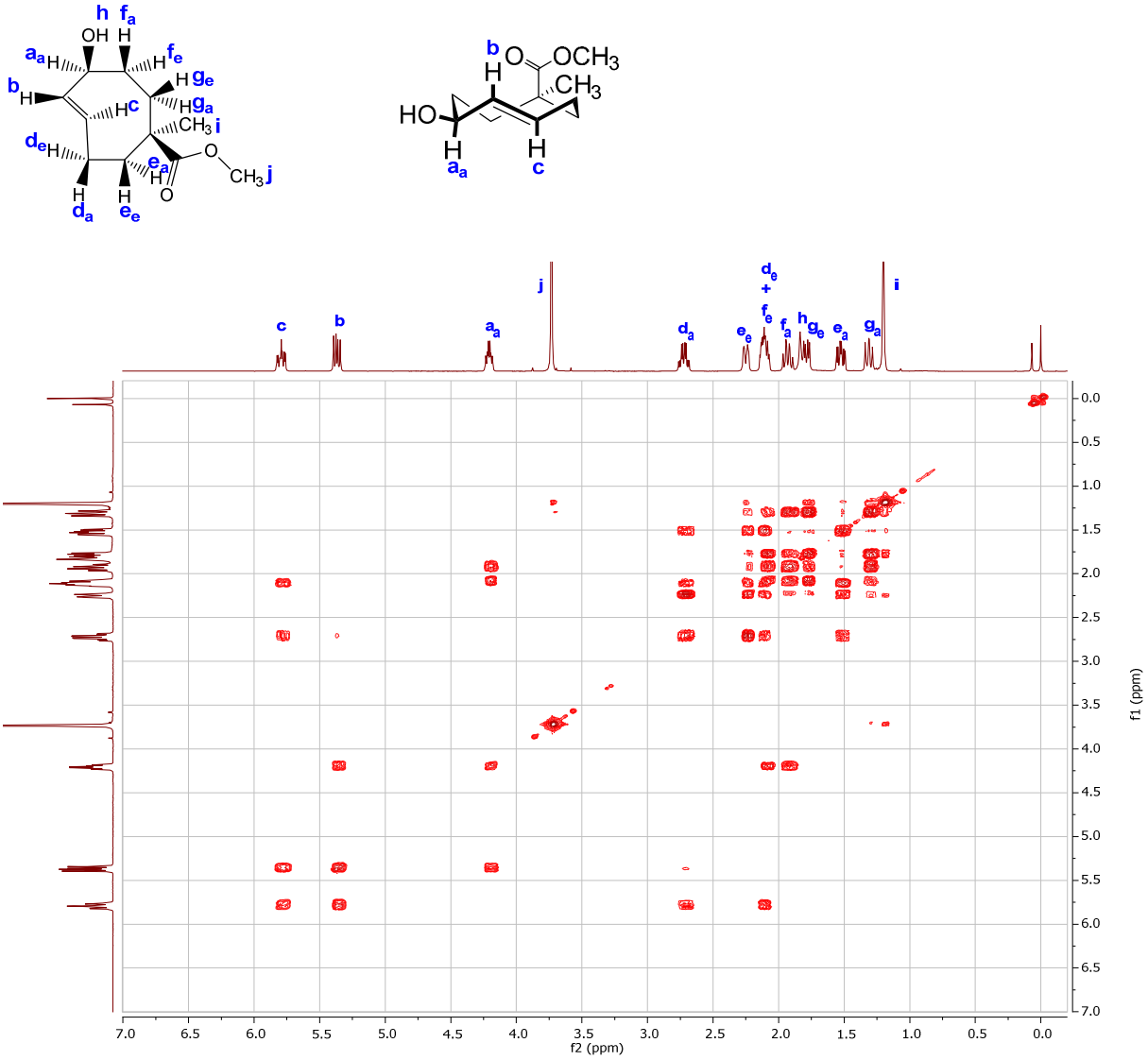

HSQC spectrum of methyl *rel*-(1*S*,6*S*,4*E*,*pS*)-6-hydroxy-1-methylcyclooct-4-ene-1-carboxylate (equatorial isomer 20b) (500 MHz, $CDCl_3$)

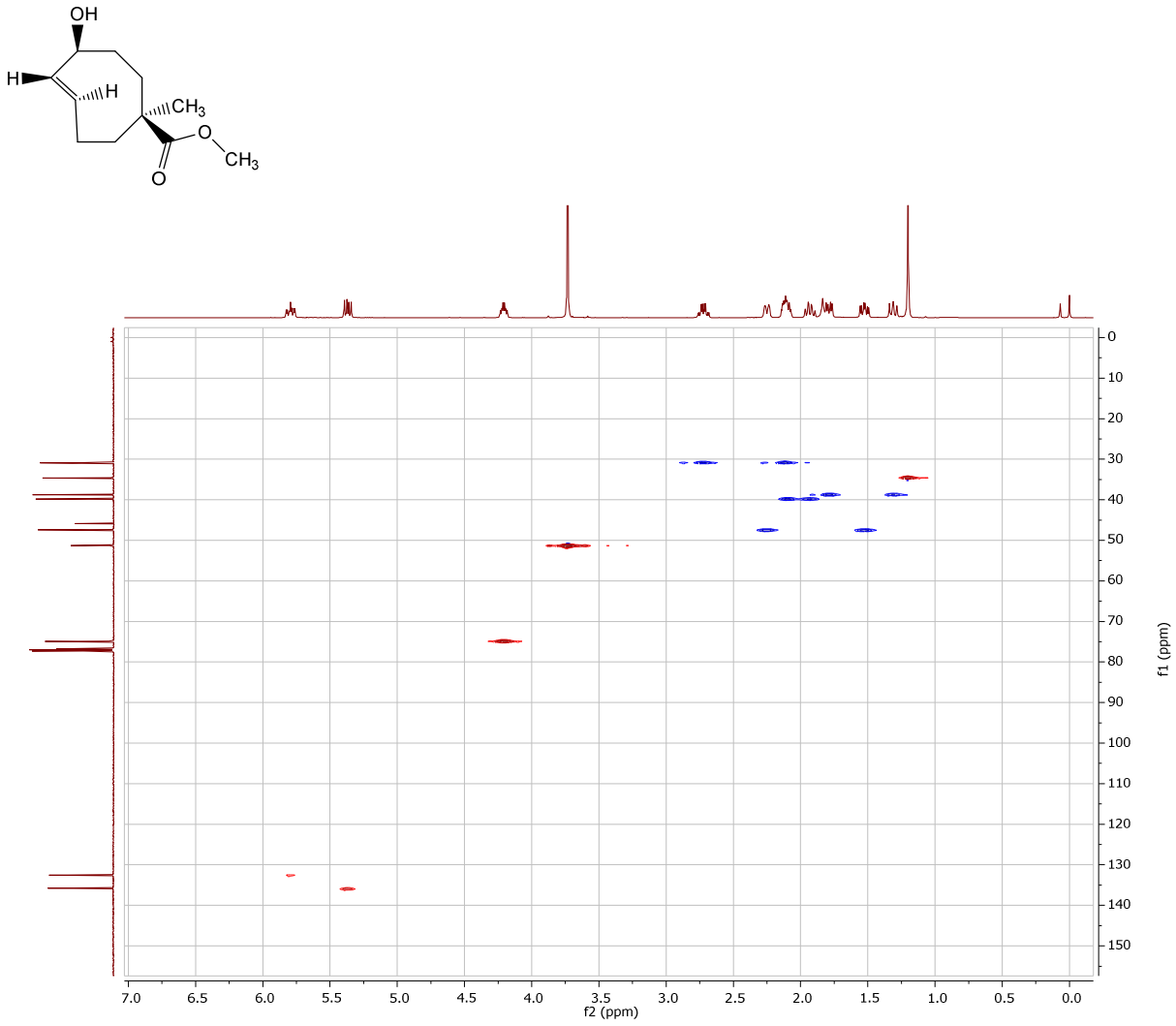

1D-NOESY spectra of methyl *rel*-(1*S*,6*S*,4*E*,*pS*)-6-hydroxy-1-methylcyclooct-4-ene-1-carboxylate (equatorial isomer 20b) (500 MHz, $CDCl_3$)

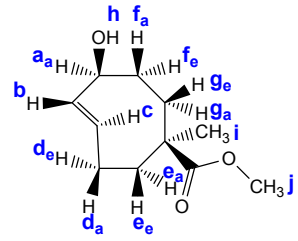

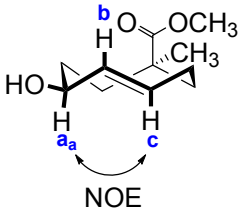

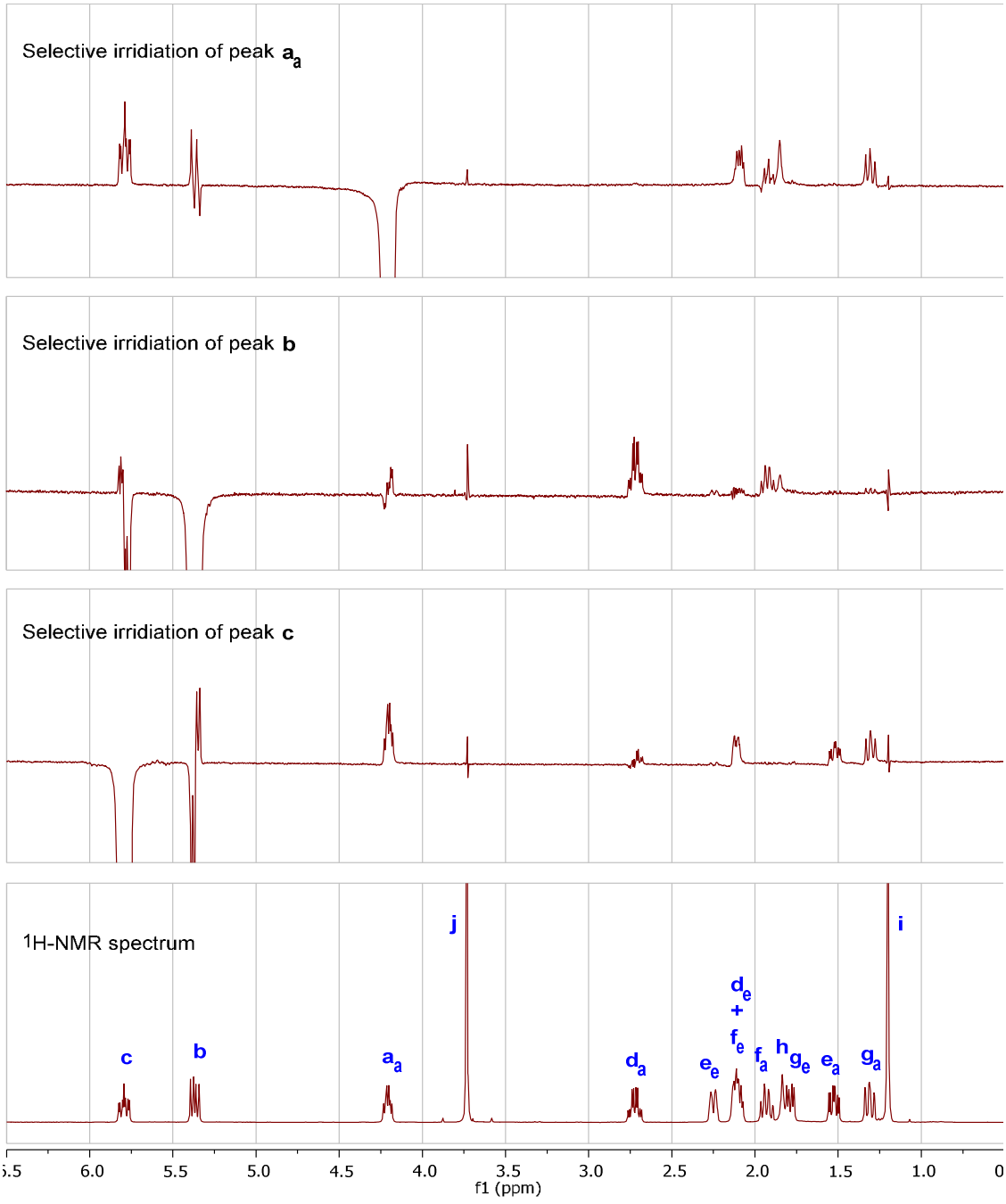

^{1}H-NMR spectrum of *rel*-(1*R*,4*E*,6*R*,*pS*)-6-hydroxy-1-methylcyclooct-4-ene-1-carboxylic acid (axial isomer 21a) (300 MHz, $CDCl_3$)

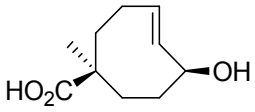

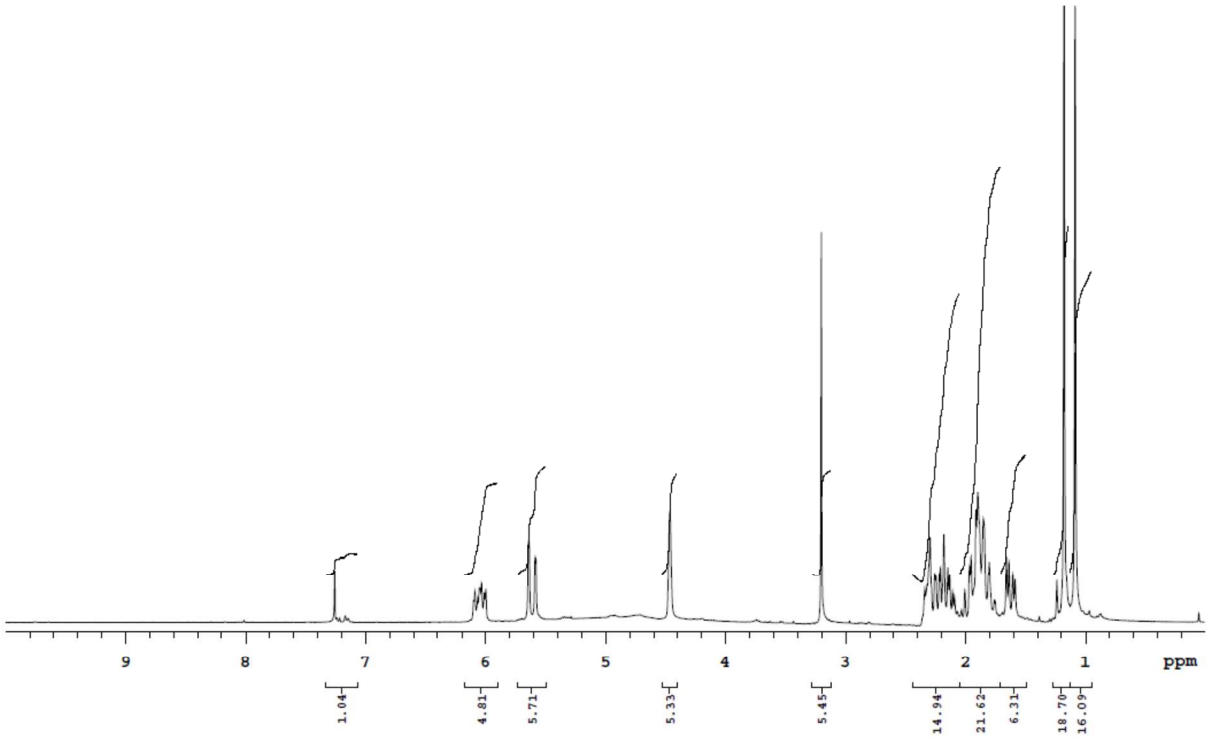

^{1}H-NMR spectrum of *rel*-(1*R*,4*E*,6*R*,*pS*)-2,5-dioxopyrrolidin-1-yl-6-((((2,5-dioxopyrrolidin-1-yl)oxy)carbonyl)oxy)-1-methylcyclooct-4-ene-1-carboxylate (axial isomer 22a) (400 MHz, $CDCl_3$)

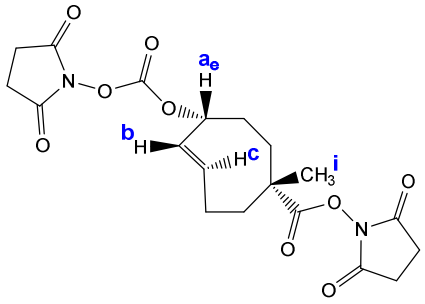

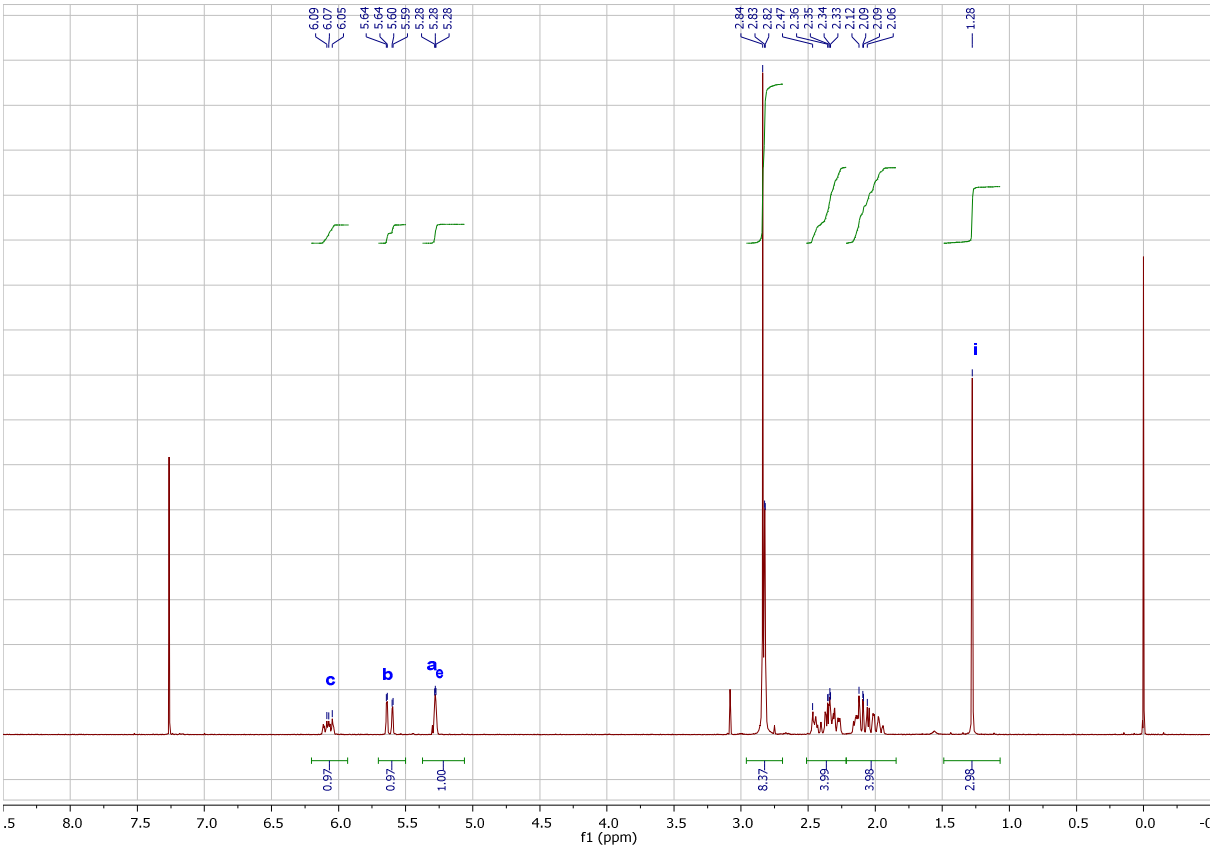

^{13}C-NMR spectrum of *rel*-(1*R*,4*E*,6*R*,*pS*)-2,5-dioxopyrrolidin-1-yl-6-((((2,5-dioxopyrrolidin-1-yl)oxy)carbonyl)oxy)-1-methylcyclooct-4-ene-1-carboxylate (axial isomer 22a) (100 MHz, $CDCl_3$)

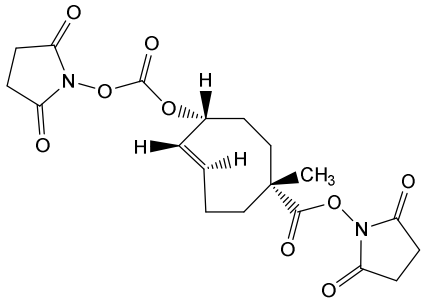

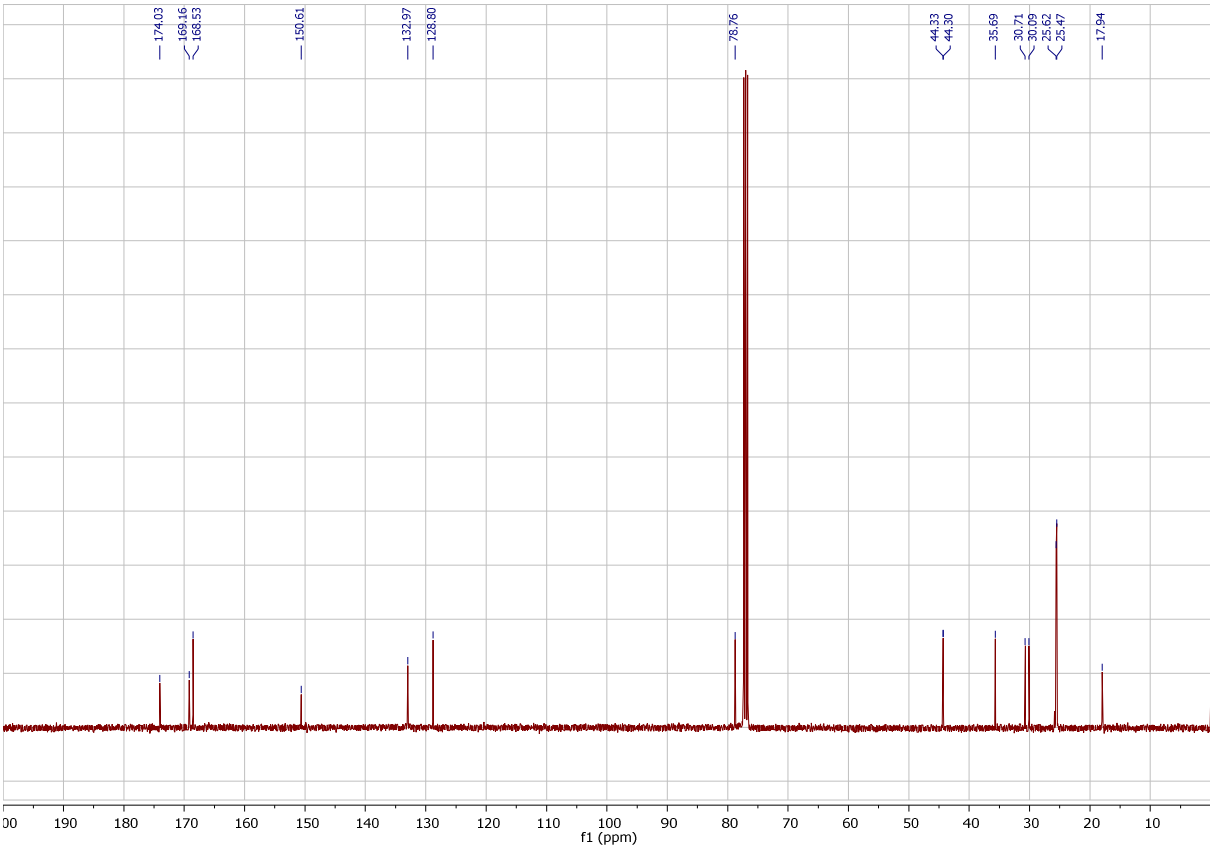

COSY spectrum of *rel*-(1*R*,4*E*,6*R*,*pS*)-2,5-dioxopyrrolidin-1-yl-6-((((2,5-dioxopyrrolidin-1-yl)oxy)carbonyl)oxy)-1-methylcyclooct-4-ene-1-carboxylate (axial isomer 22a) (400 MHz, $CDCl_3$)

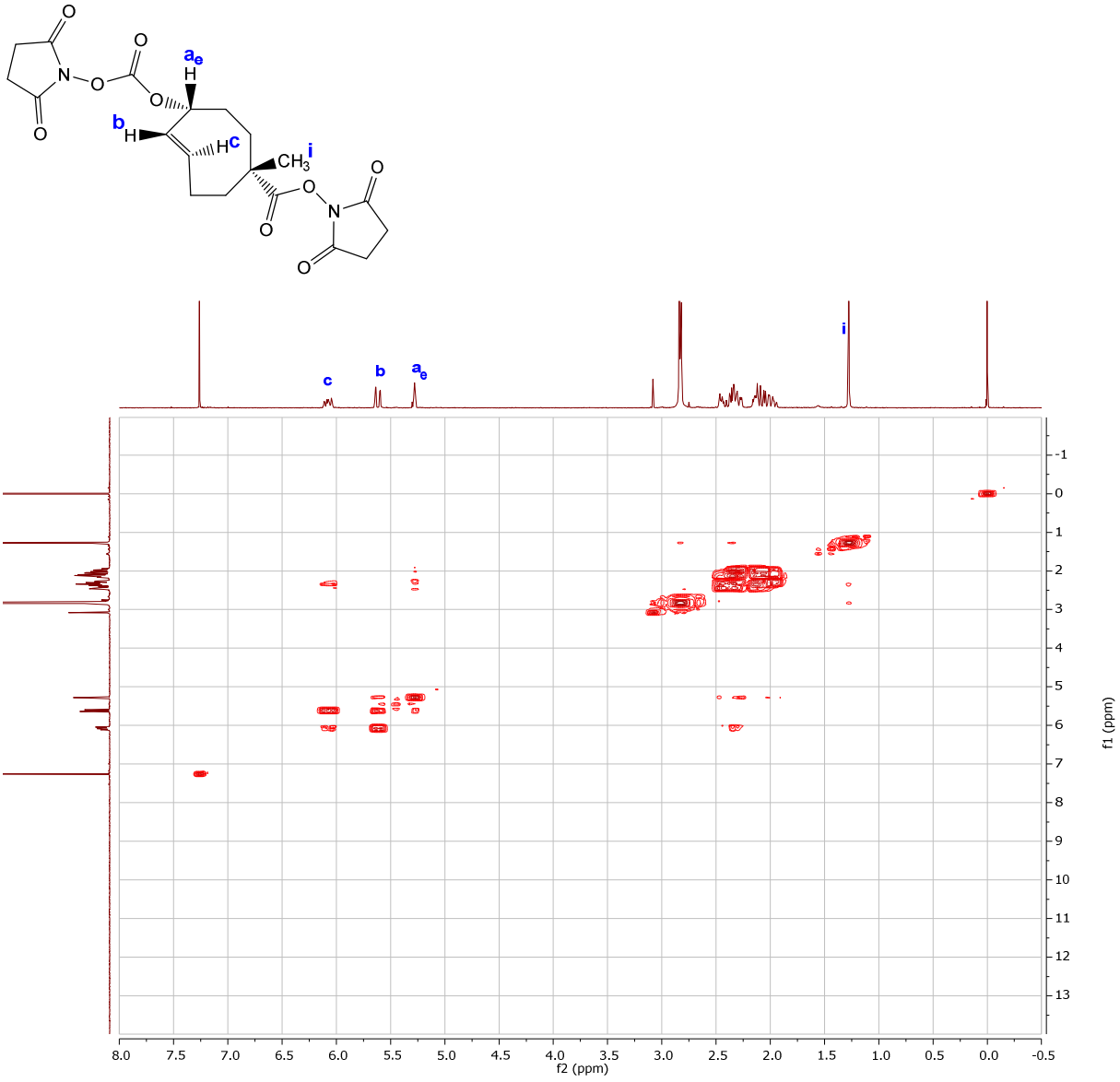

1D-NOESY spectra of *rel*-(1*R*,4*E*,6*R*,*pS*)-2,5-dioxopyrrolidin-1-yl-6-((((2,5-dioxopyrrolidin-1-yl)oxy)carbonyl)oxy)-1-methylcyclooct-4-ene-1-carboxylate (axial isomer 22a) (500 MHz, $CDCl_3$)

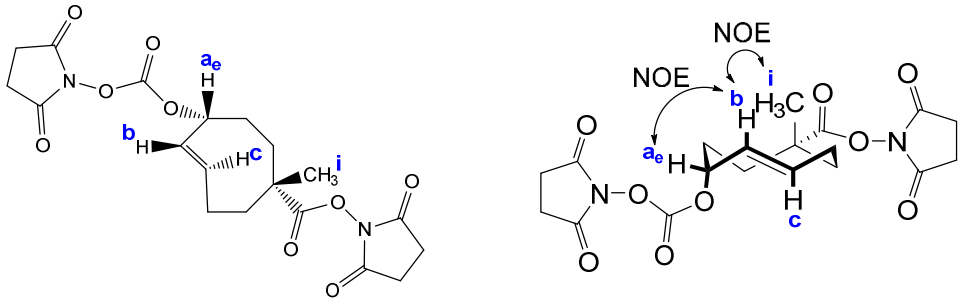

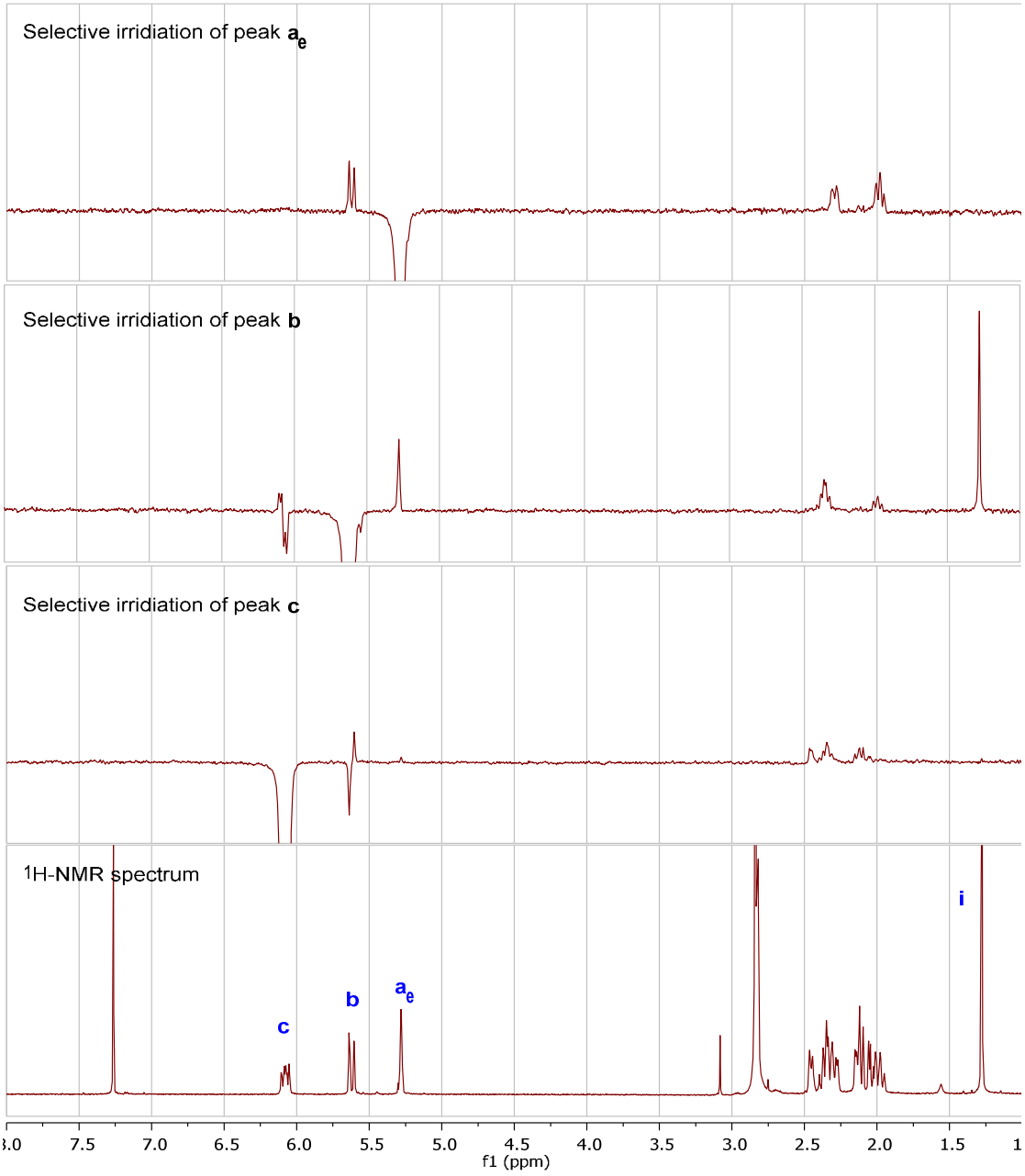

^{1}H-NMR spectrum of Dox-TCO-NHS (23a) (400 MHz, DMSO-d6)

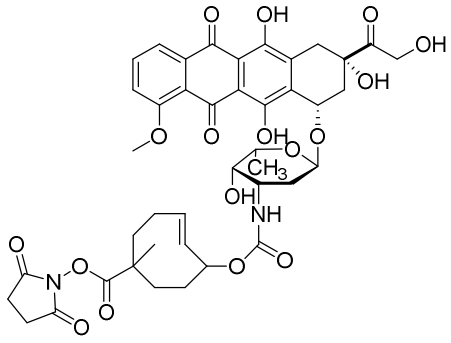

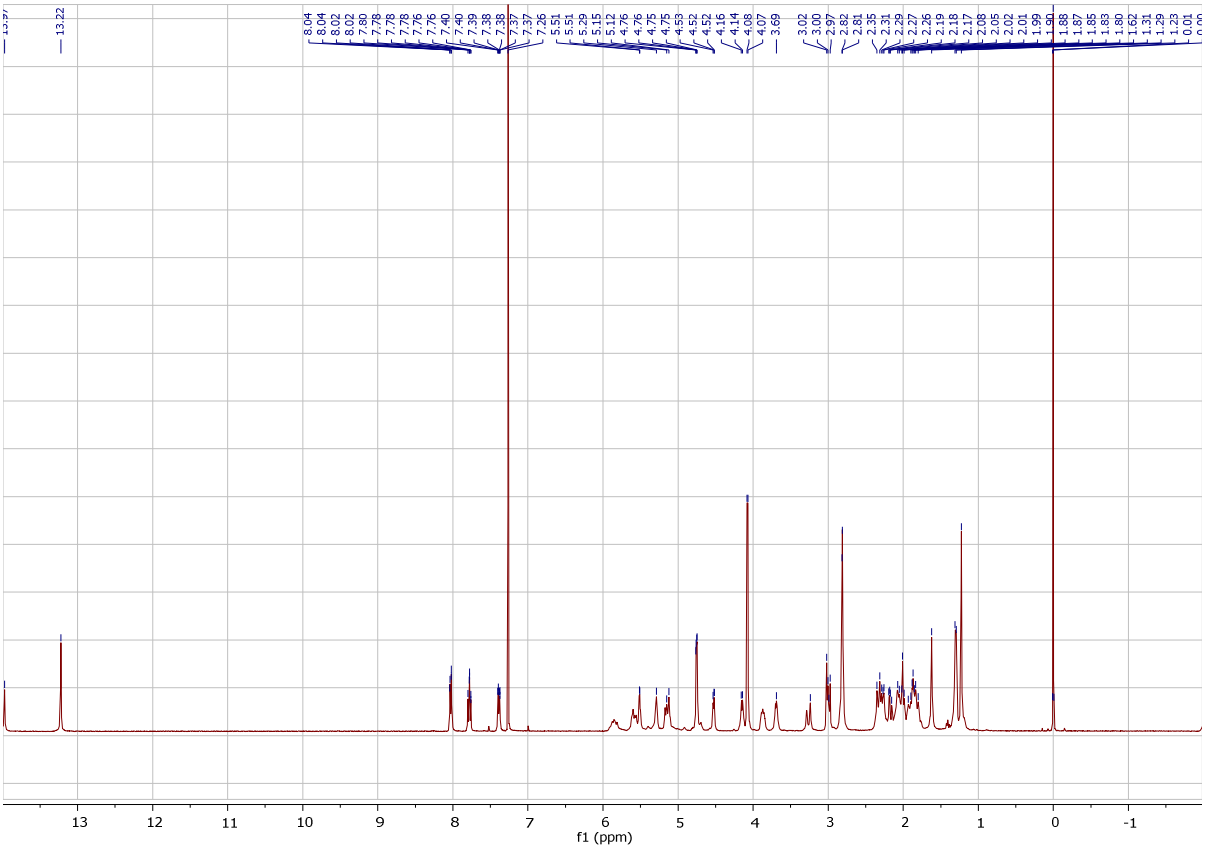

^{13}C-NMR spectrum of Dox-TCO-NHS (23a) (100 MHz, DMSO-d6)

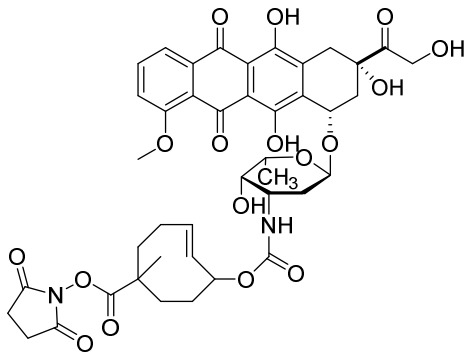

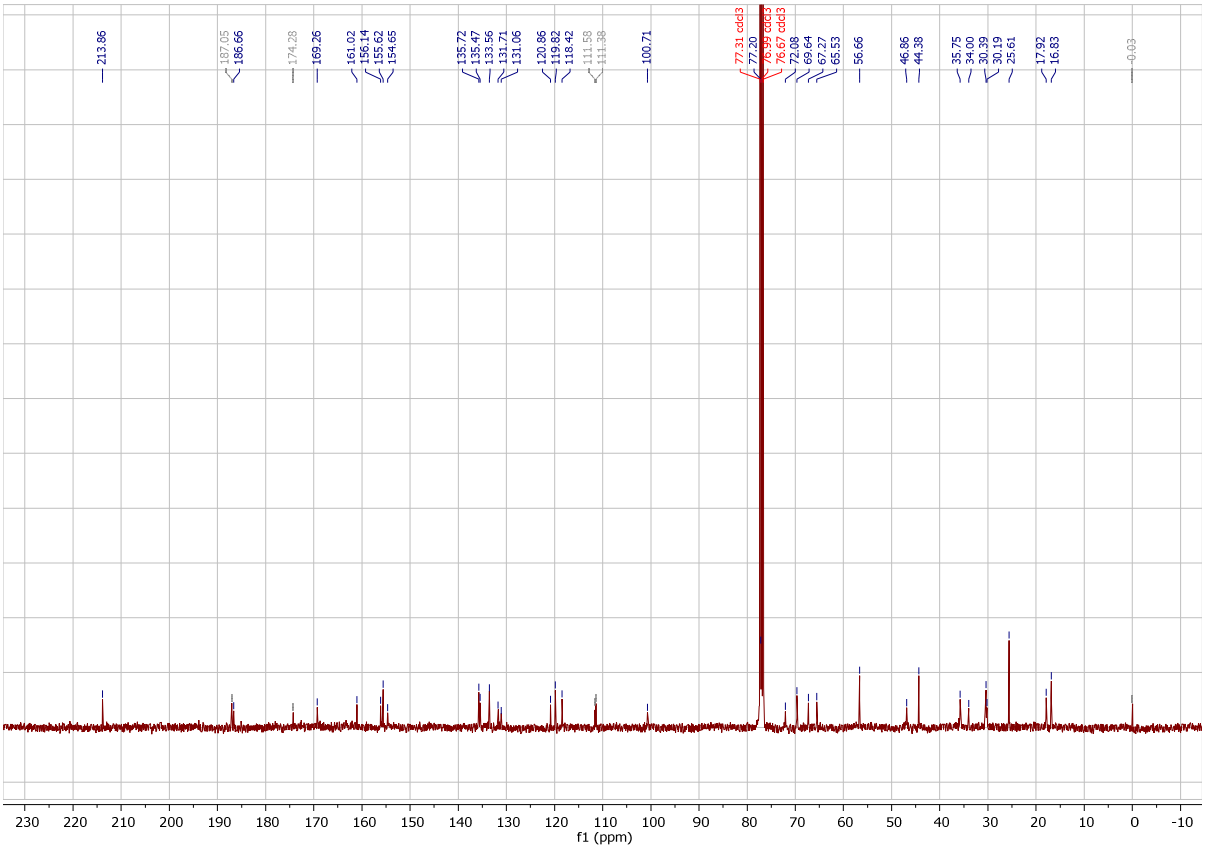

HPLC-MS chromatogram of Dox-TCO-NHS (23a)

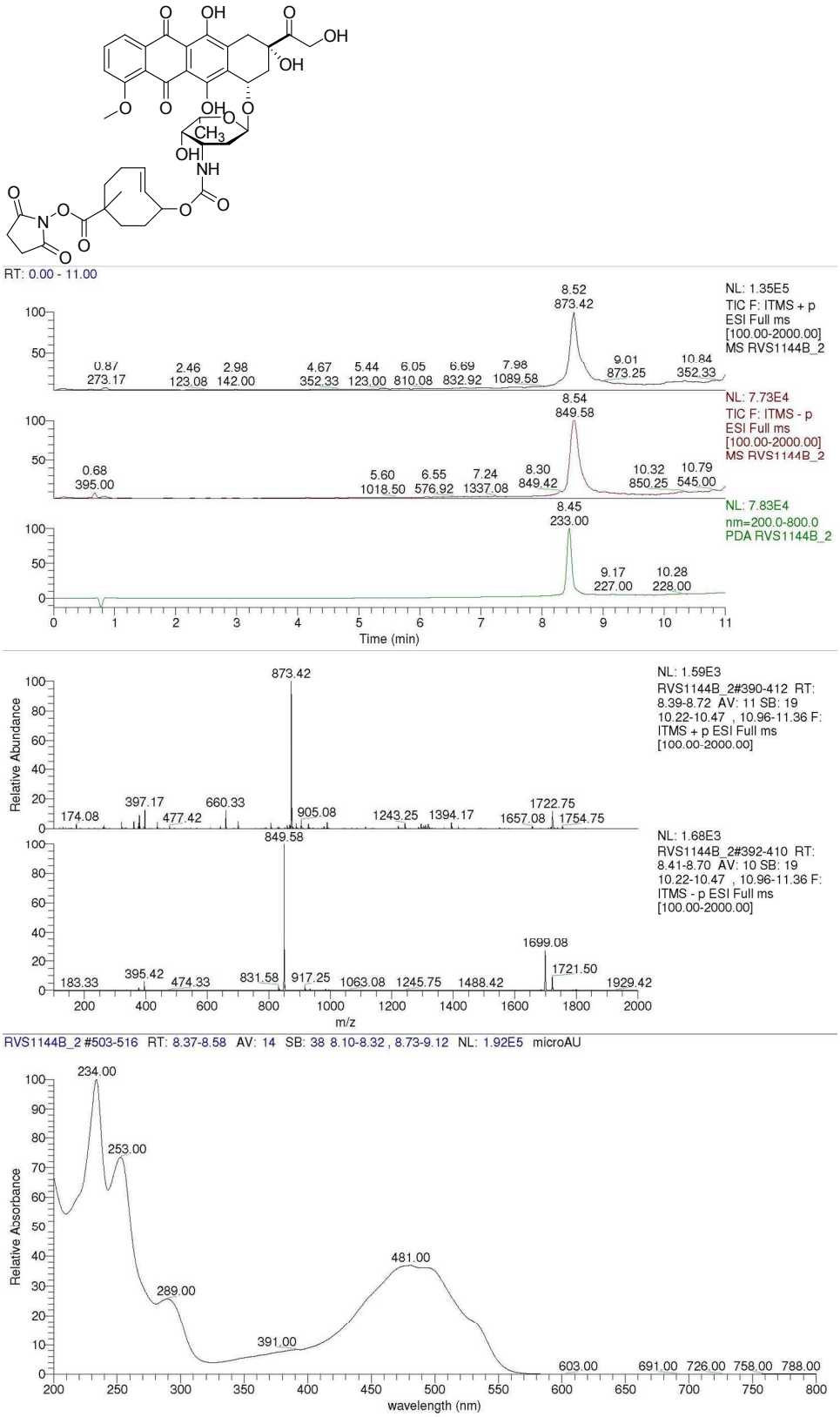

HRMS spectrum of Dox-TCO-NHS (23a)

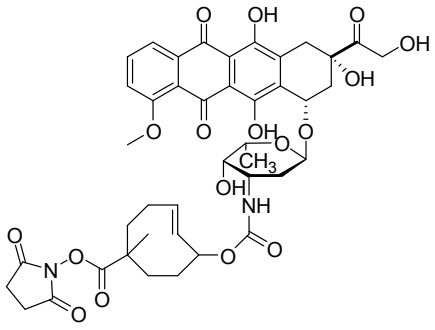

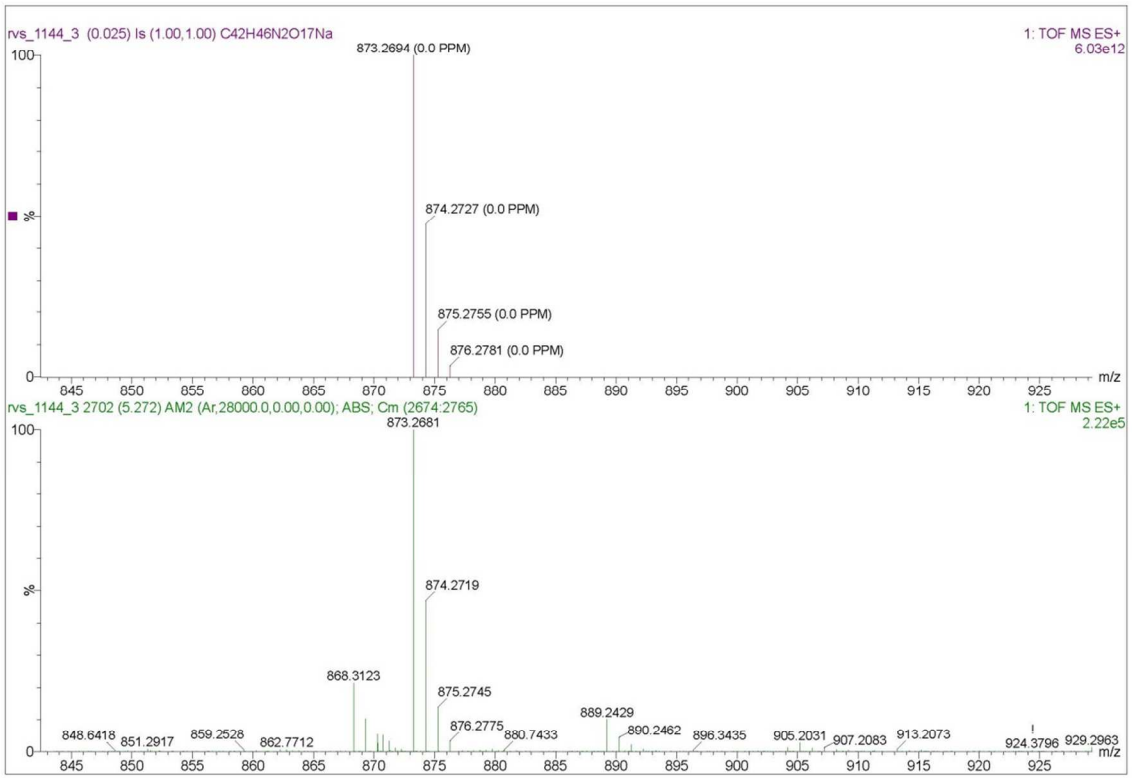

HPLC-MS/PDA spectra demonstrating tetrazine (3)-induced release of Doxorubicin from NHS-TCO-Doxorubicin (axial isomer 23a)

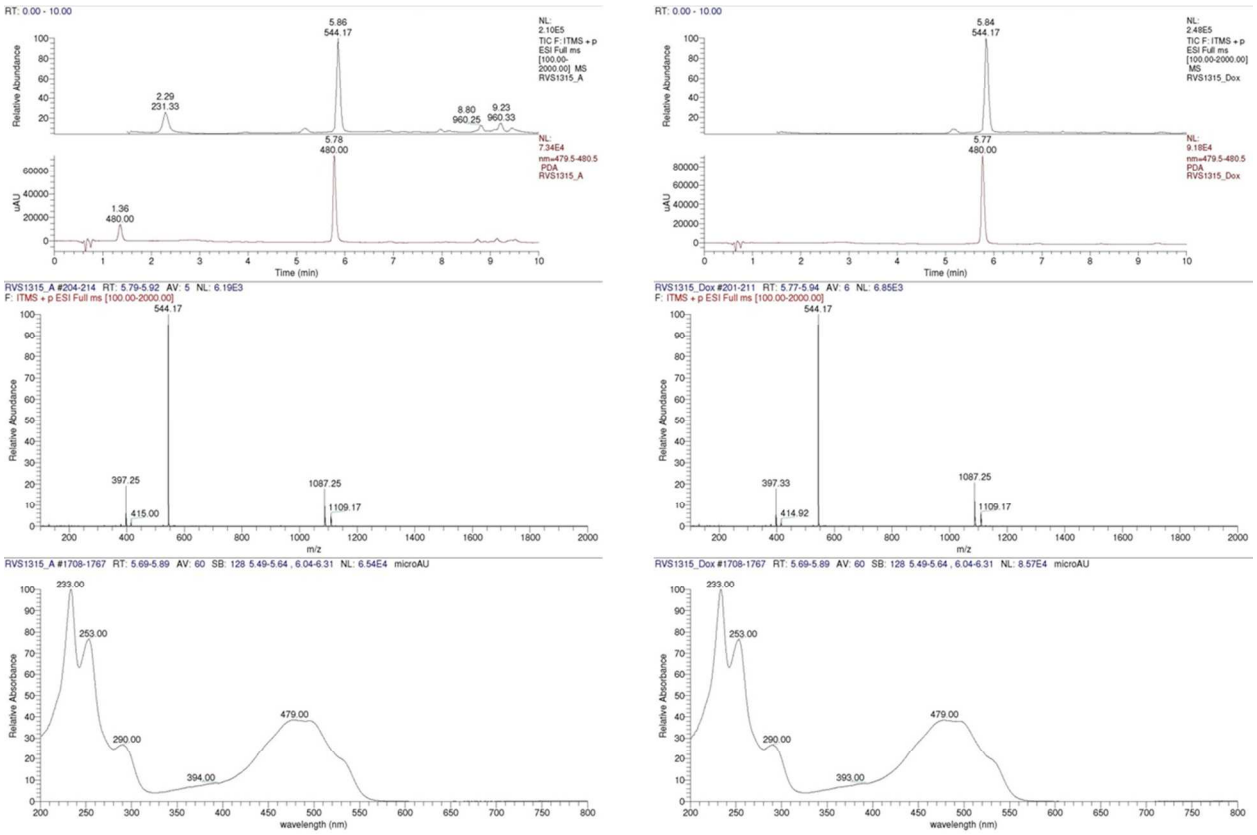

Left: HPLC-MS/PDA from reaction mixture after 60 min at 37°C. Right: HPLC-MS/PDA from a control sample of Doxorubicin.HCl

^{1}H-NMR spectrum of 3-(tert-butoxycarbonylaminomethyl)-6-methyl-1,2,4,5-tetrazine (24) (400 MHz, $CDCl_3$)

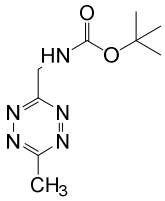

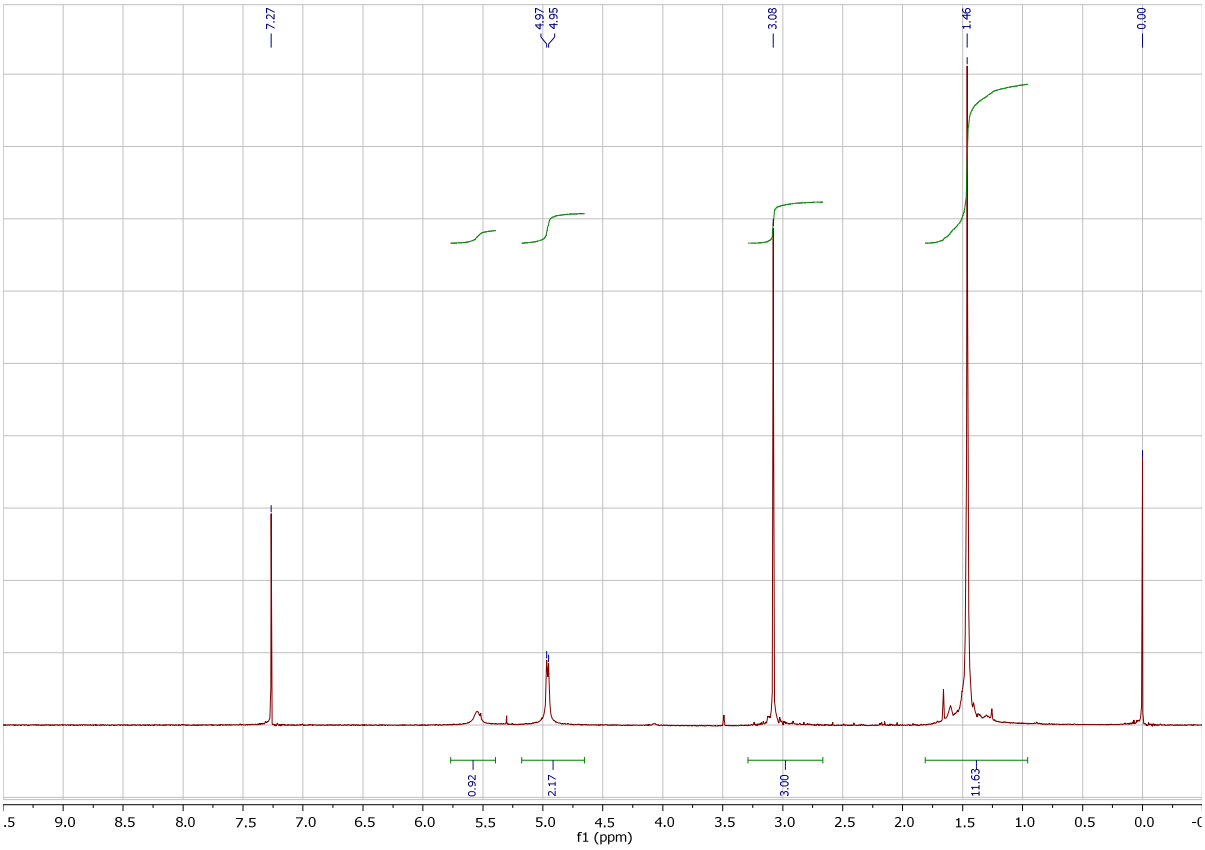

HPLC-MS chromatogram of 3-(tert-butoxycarbonylaminomethyl)-6-methyl-1,2,4,5-tetrazine (24)

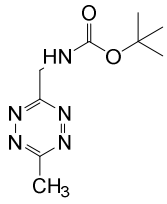

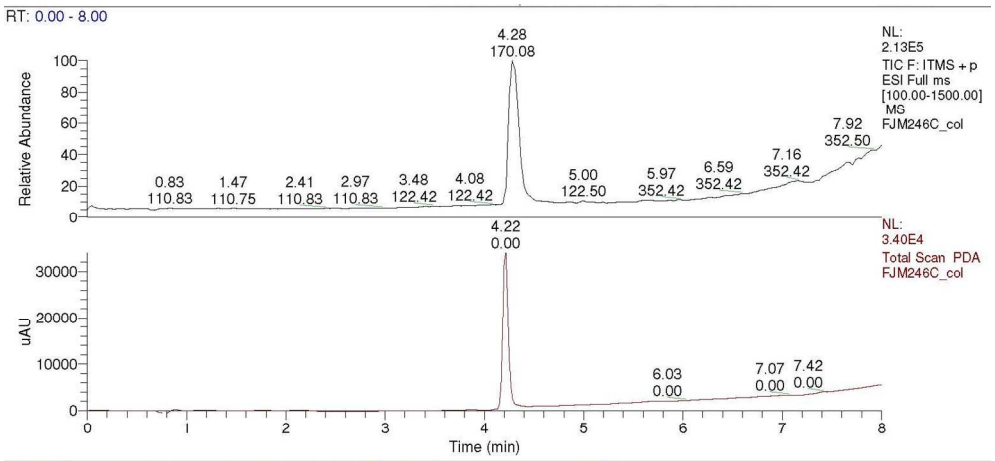

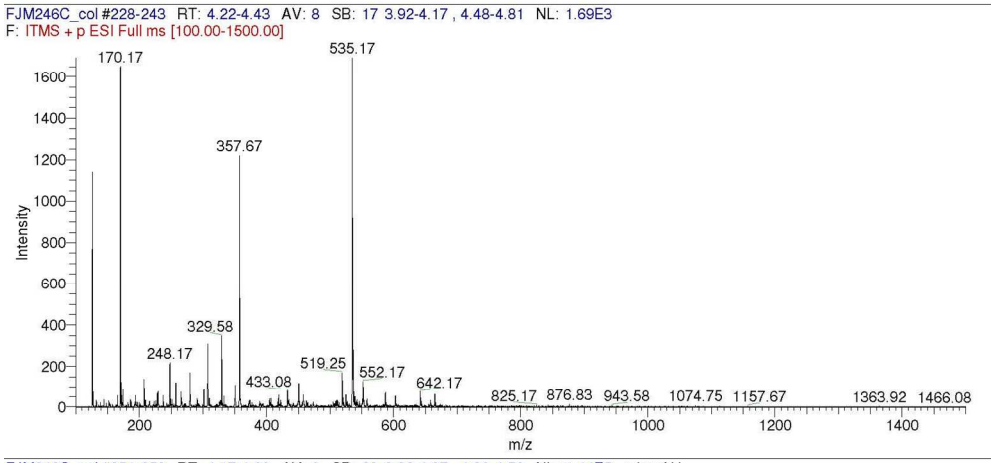

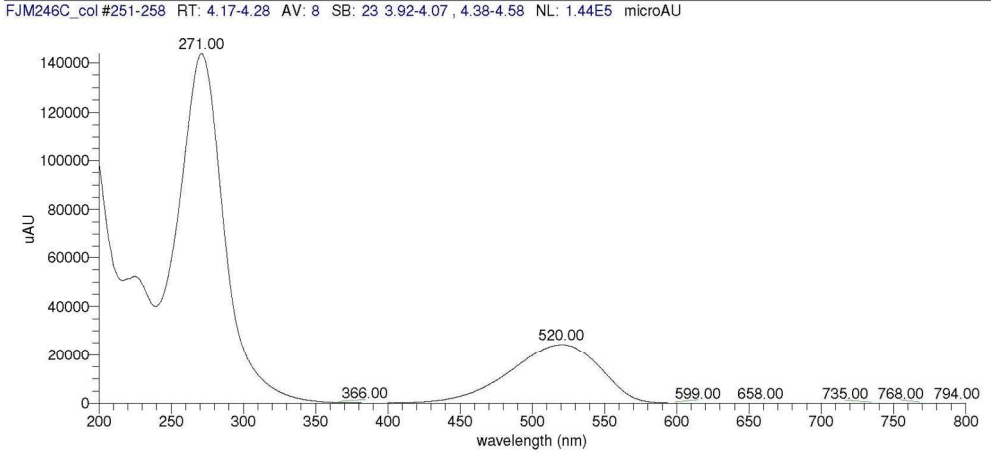

^{1}H-NMR spectrum of 5-(((6-methyl-1,2,4,5-tetrazin-3-yl)methyl)amino)-5-oxopentanoic acid (26) (400 MHz, MeOD-d4)

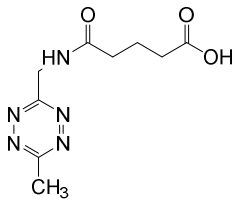

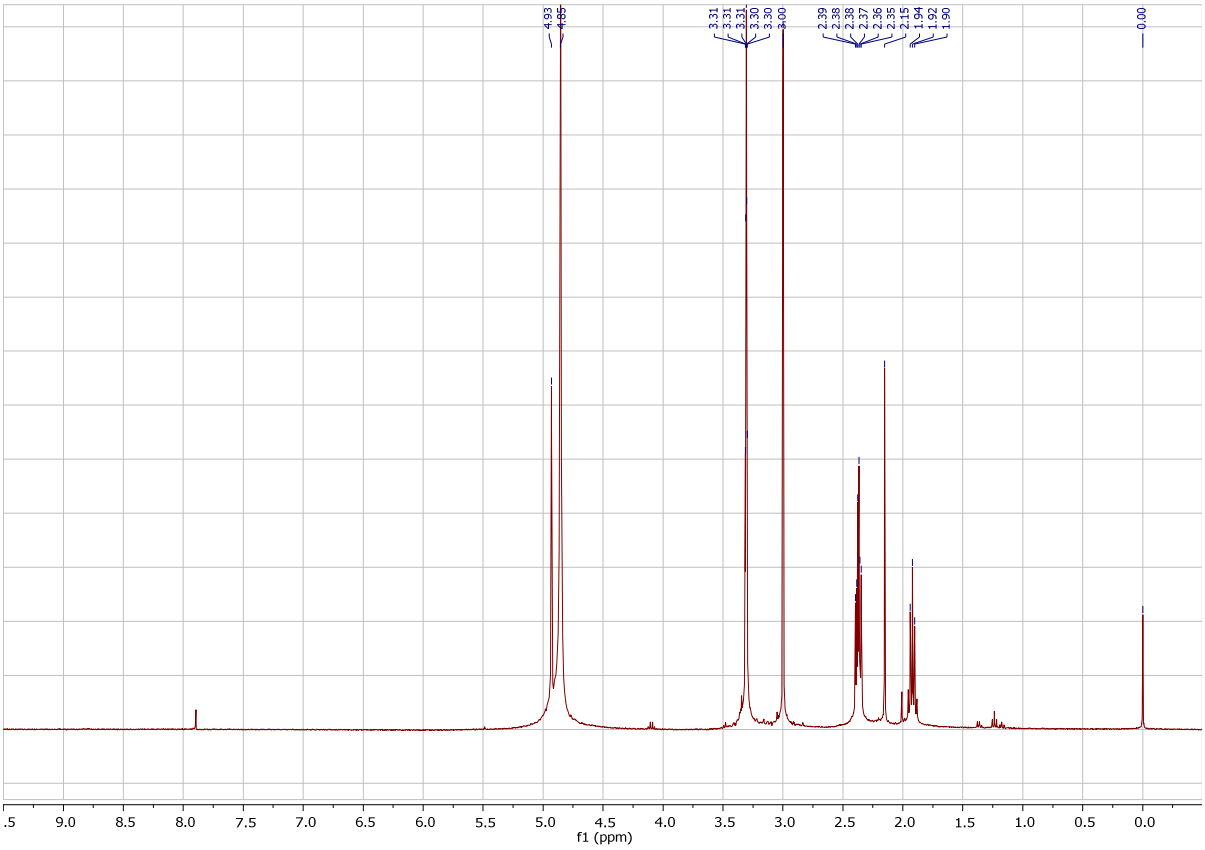

^{13}C-NMR spectrum of 5-(((6-methyl-1,2,4,5-tetrazin-3-yl)methyl)amino)-5-oxopentanoic acid (26) (100 MHz, MeOD-d4)

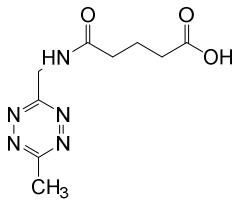

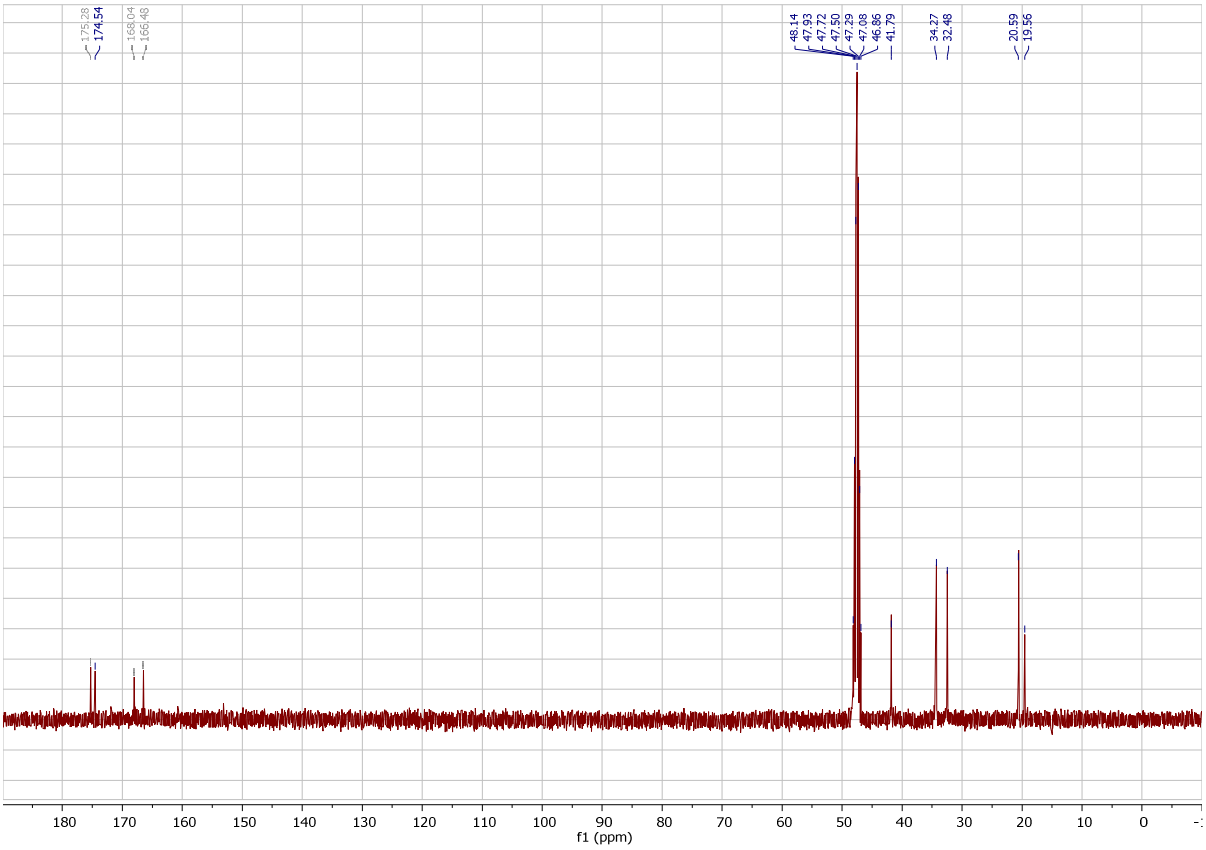

HPLC-MS chromatogram of 5-(((6-methyl-1,2,4,5-tetrazin-3-yl)methyl)amino)-5-oxopentanoic acid (26)

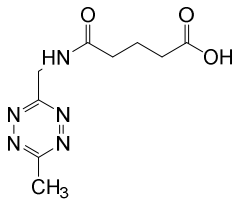

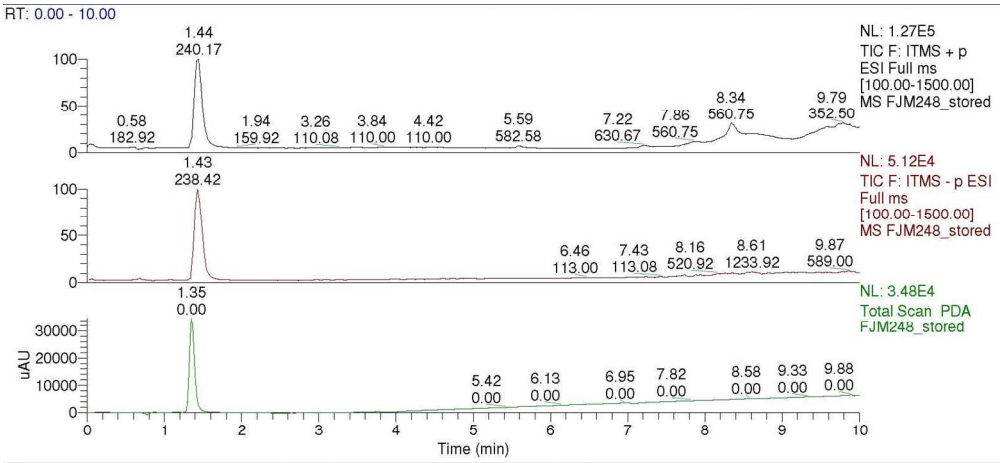

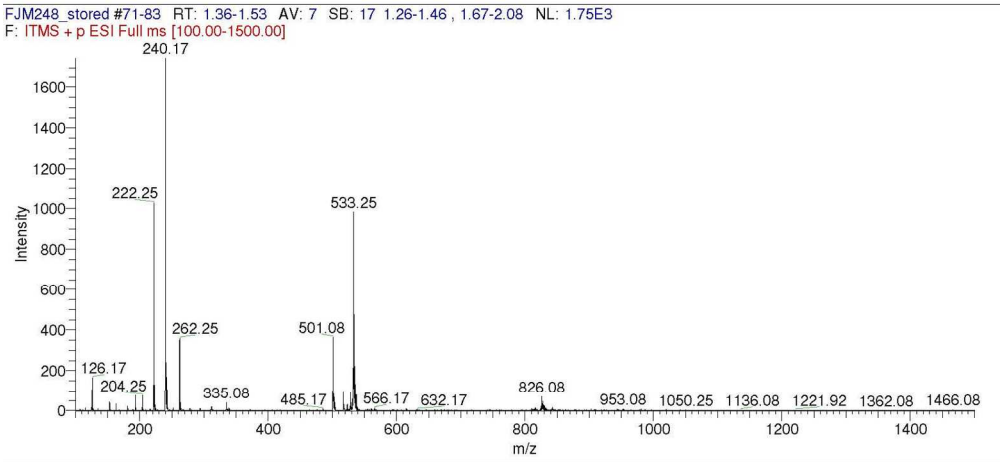

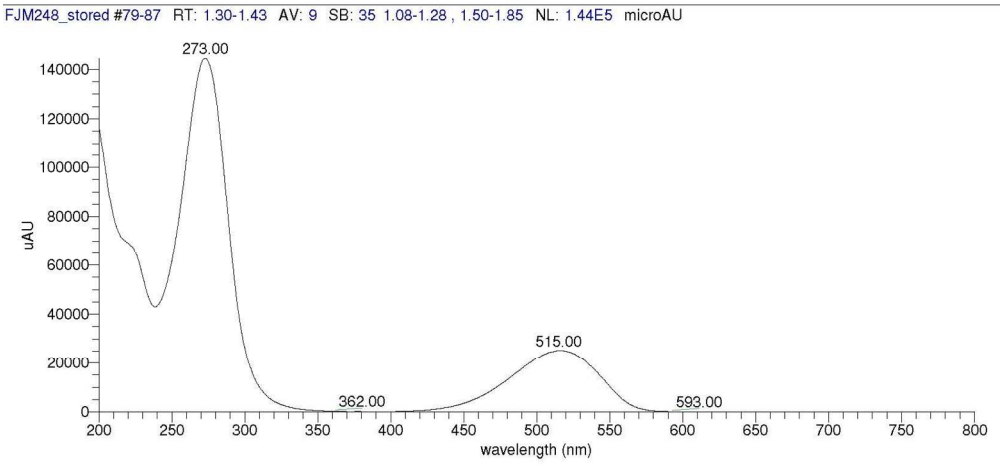

^{1}H-NMR spectrum of 3,6-dimethyl-1,2,4,5-tetrazine functional dextran (5) (400 MHz, D_2O)

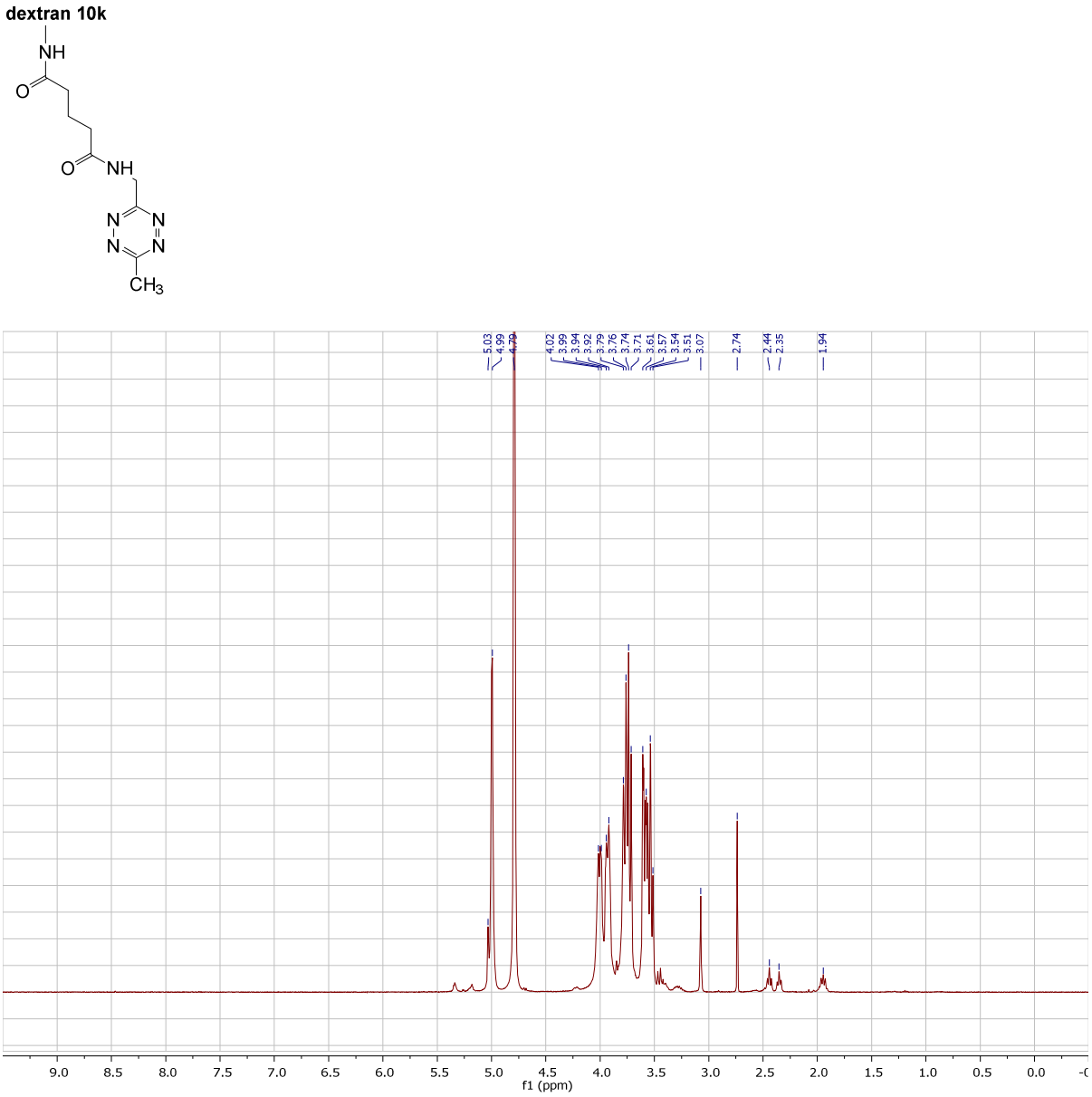

^{1}H-NMR spectrum of 5-((6-cyanopyridin-3-yl)amino)-5-oxopentanoic acid (27) (400 MHz, DMSO-d6)

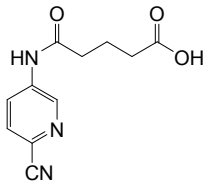

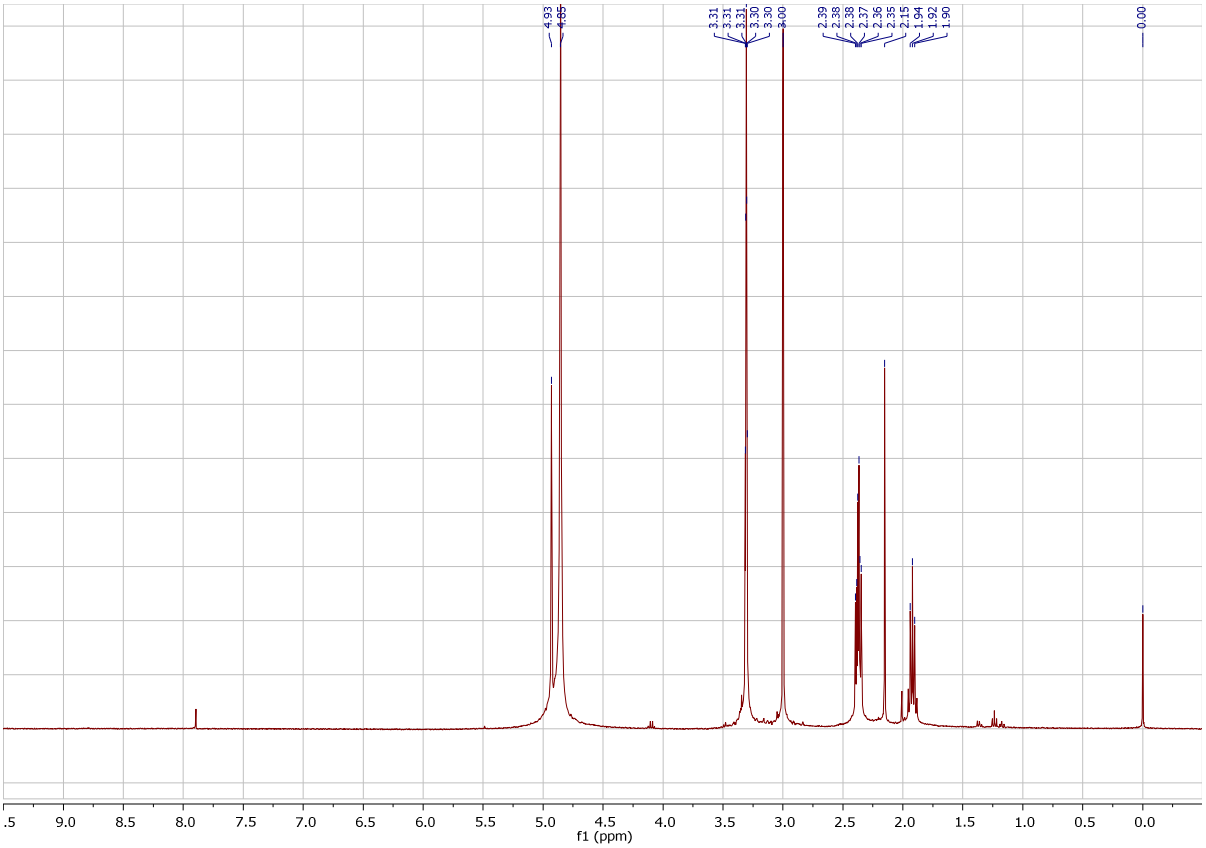

^{13}C-NMR spectrum of 5-((6-cyanopyridin-3-yl)amino)-5-oxopentanoic acid (27) (400 MHz, DMSO-d6)

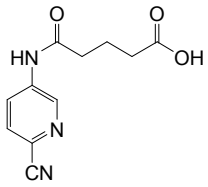

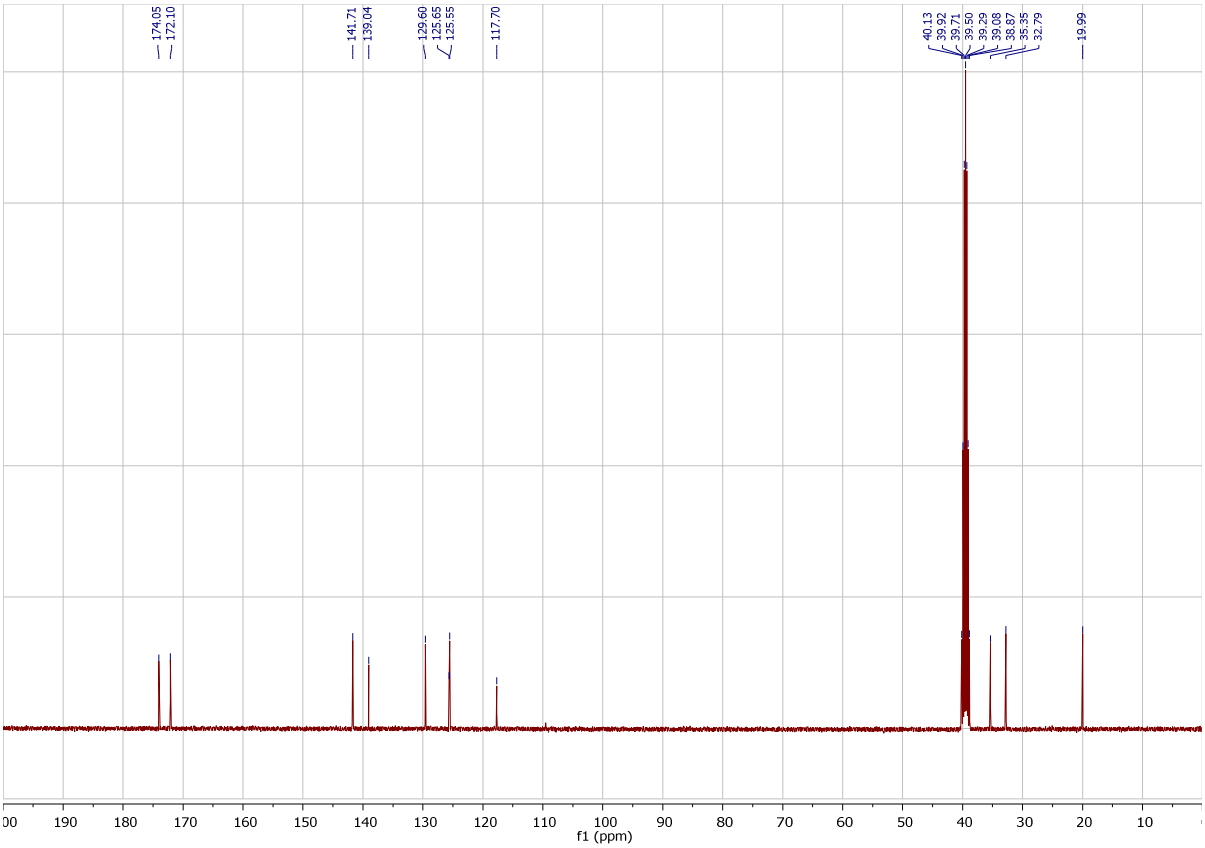

HPLC-MS chromatogram of 5-((6-cyanopyridin-3-yl)amino)-5-oxopentanoic acid (27)

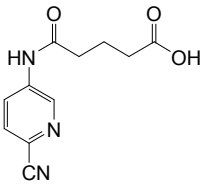

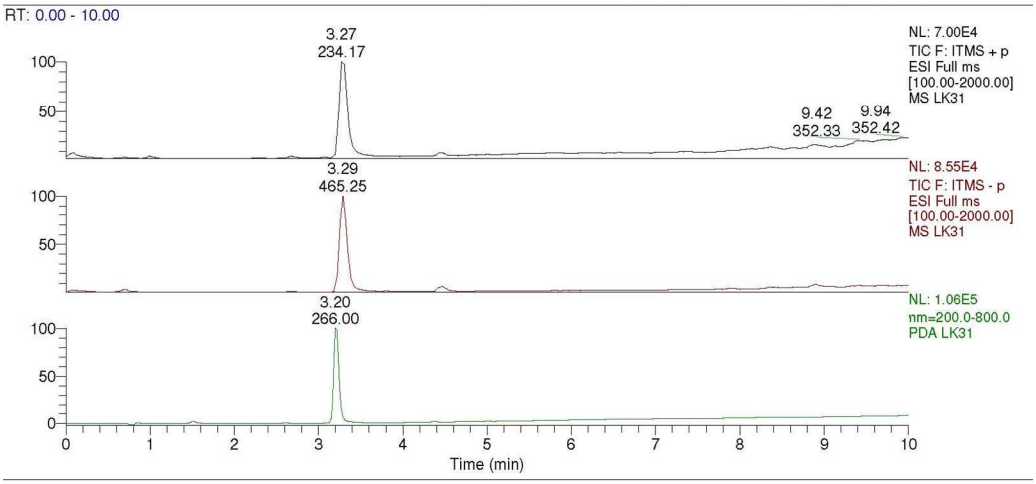

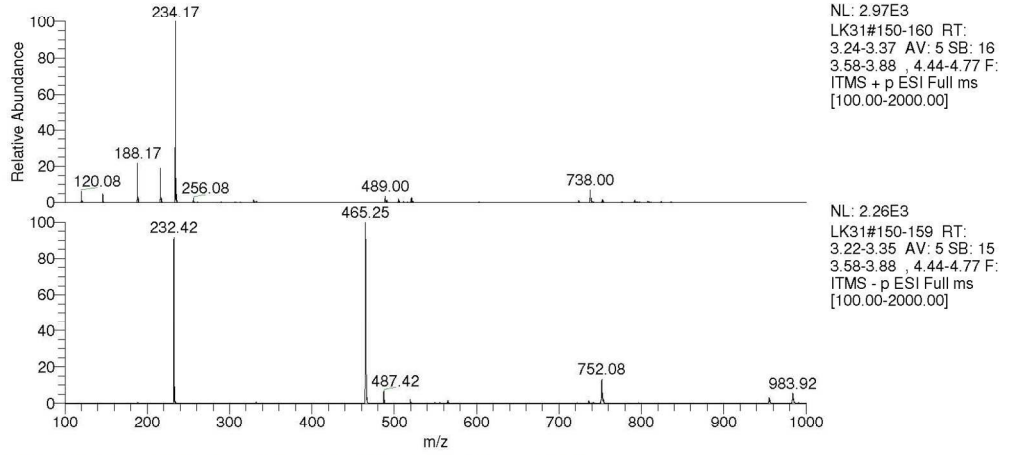

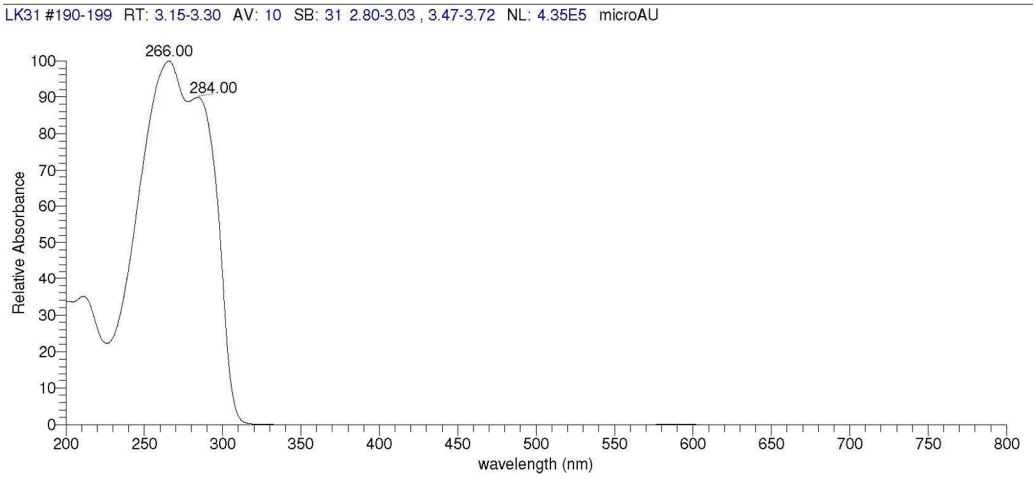

^{1}H-NMR spectrum of 5-((6-(6-methyl-1,2,4,5-tetrazin-3-yl)pyridin-3-yl)amino)-5-oxopentanoic acid (28) (400 MHz, DMSO-d6)

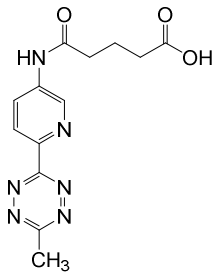

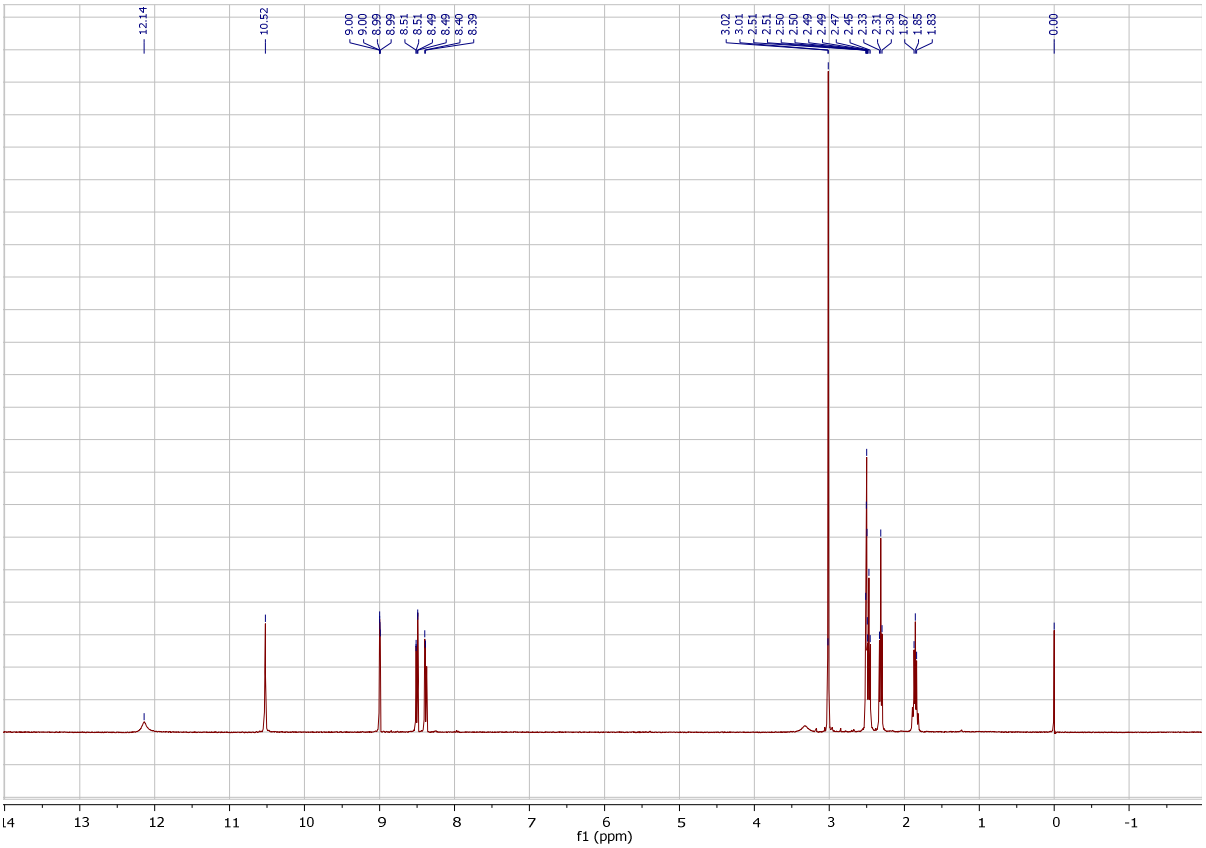

^{13}C-NMR spectrum of 5-((6-(6-methyl-1,2,4,5-tetrazin-3-yl)pyridin-3-yl)amino)-5-oxopentanoic acid (28) (100 MHz, DMSO-d6)

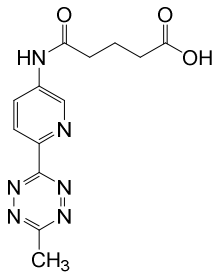

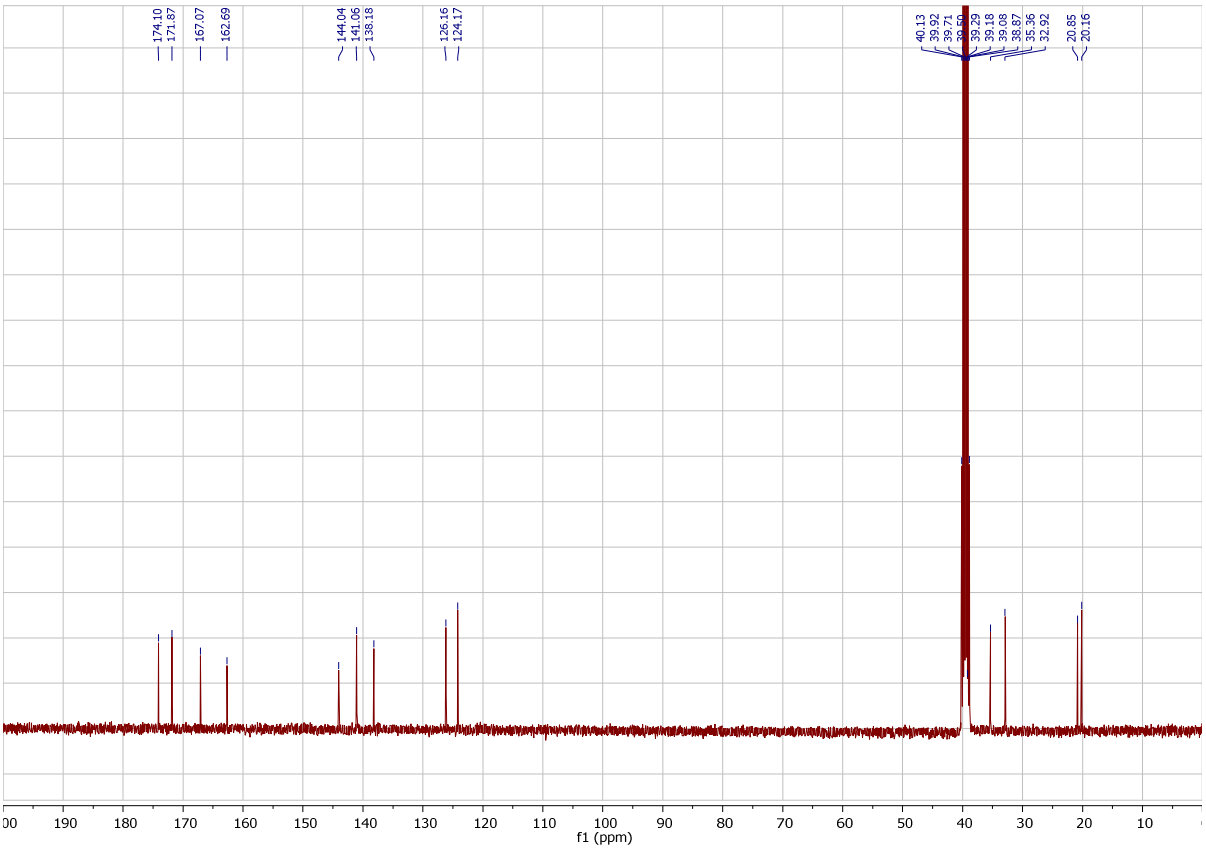

HPLC-MS chromatogram of 5-((6-(6-methyl-1,2,4,5-tetrazin-3-yl)pyridin-3-yl)amino)-5-oxopentanoic acid (28)

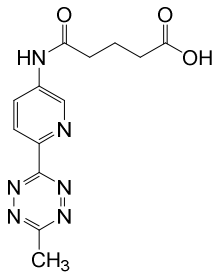

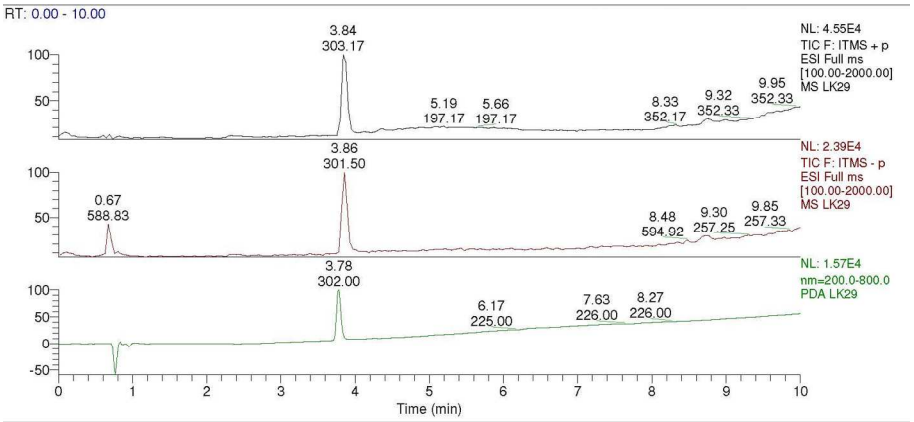

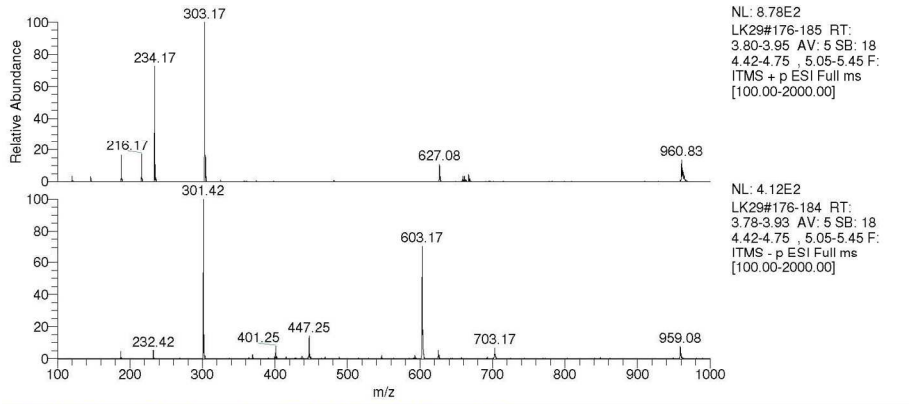

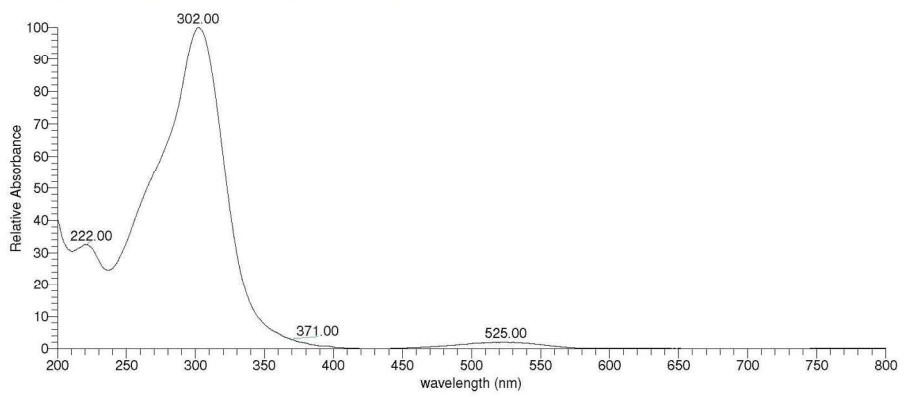

^{1}H-NMR spectrum of 3-(pyridin-2-yl)-6-methyl-1,2,4,5-tetrazine functional dextran (6) (400 MHz, D_2O)